A MODEL–BASED STUDY OF A CURVED AND SKEWED SLAB TYPE BRIDGE DECK USED IN MAKKAH

BY

FARHAT ABDUL-MUNIM ISAILI

A Thesis Presented to the

DEANSHIP OF GRADUATE STUDIES

KING FAHD UNIVERSITY OF PETROLEUM & MINERALS

DHAHRAN, SAUDI ARABIA

In Partial Fulfillment of the
Requirements for the Degree of

MASTER OF SCIENCE

In

CIVIL ENGINEERING

May, 2011

KING FAHD UNIVERSITY OF PETROLEUM & MINERALS
DHAHRAN 31261, SAUDI ARABIA

DEANSHIP OF GRADUATE STUDIES

This thesis, written by **Farhat Abdul Munim Isaili** under the direction of his thesis advisor and approved by his thesis committee, has been presented to and accepted by the Dean of Graduate Studies, in partial fulfillment of the requirements for the degree of **MASTER OF SCIENCE** IN **CIVIL ENGINEERING**

Thesis Committee

Prof. Abul Kalam Azad (Advisor)

Prof. Muhammed Baluch (Co-Advisor)

Dr. Muhammed Kalimur Rahman (Member)

Dr. Ali Algadhib (Member)

Dr. Mustafa Almandil (Member)

Dr. Nedal T. Ratrout 13 JUN 2011
(Department Chairman)

Dr. Salam A. Zummo
(Dean of Graduate Studies)

15/6/11
Date

عمادة الدراسات العليا
DEANSHIP OF GRADUATE STUDIES

DEDICATED
TO MY FATHER, MOTHER, WIFE AND MY CHILD AND TO MY BROTHERS AND SISTERS

ACKNOWLEDGMENT

All praise and thanks are due to my Lord, ALLAH SUBHANHO WA TAALA, for giving me the health, knowledge and patience to complete this work. I acknowledge the financial support given by KFUPM's Civil Engineering Department during my graduate studies.

My sincerest gratitude goes to my advisor Prof. Abul Kalam Azad and co-advisor Prof. Muhammed Baluch who guided me with their dedicated attention, expertise, and knowledge throughout this research. I am also grateful to my Committee Members, Dr. Ali Algadhib, Dr. Mustafa Al-Mandil and Dr. Muhammad Kalimur Rahman, for their constructive guidance and support. Thanks are also due to the department's Chairman Dr. Nedal T. Ratrout and his secretary for providing aid, and to other staff members of the department who helped me directly or indirectly.

Special thanks are due to my colleagues in the Civil Engineering Department, for their aid and support. Thanks are also due to all my friends for their support and encouragement specially Murad Abu Saleimah, Muhammad Al Osta And Abdullah Al Ghamdi.

My heartfelt gratitude is given to my beloved father, mother, my wife Arwa and my child Salahuddin, whom always support me with their love, patience, encouragement and constant prayers. I would like to thank my brothers, sisters, and all members of my family in Palestine for their emotional and moral support throughout my study.

TABLE OF CONTENTS

ACKNOWLEDGMENT iii

TABLE OF CONTENTS iv

LIST OF TABLES vii

LIST OF FIGURES viii

THESIS ABSTRACT.....xi
THESIS ABSTRACT(ARABIC).....xiii

CHAPTER ONE 1

1 INTRODUCTION.....1

1.1 General 1
1.2 Needs for this Research.....5
1.3 Objectives and Scope of research 6
1.4 Reseach Methodology.....7

CHAPTER TWO.....11

2 LITERATURE REVIEW.....11

CHAPTER THREE.....19

3 THEORETICAL STUDY OF ACTUAL BRIDGE.....19

3.1 Modeling of the Bridge Deck.....19
3.2 Loads on the Slab Deck.....21
3.2.1 Dead Loads.....21
3.2.2 Live Loads.....23
3.3 Maximum Deflection in the Slab Deck.....26
3.4 Shear Stress in the Slab Deck.....27
3.5 Bending Moment Mx.....28

3.6 Bending Moment My....29
3.7 Torsional Moment Mxy 30
3.8 Principal Stress.... 31
3.9 Observations 33

CHAPTER FOUR....34

4 DEATAILS OF THE EXPERIMENTAL 34

4.1 General.... 34
4.2 Choice of Scale 34
4.3 Dead Load Factore.... 34
4.4 Live Load Factore.... 36
4.5 Model Fabrication.... 38
4.5.1 Formwork.... 38
4.5.2 Steel Work 38
4.5.3 Concrete Work.... 43
4.5.4 Support Work.... 44
4.5.5 Instrumentation 45
4.5.6 Loading.... 49
4.5.6.1 Load Cases.... 50

CHAPTER FIVE 56

5 DETAILS OF THEORETICAL FE WORK 56

5.1 General.... 56
5.2 Modeling of the Bridge Deck 56
5.3 Loads on the Slab Deck....58
5.3.1 Dead Load.... 58
5.3.2 Live Load.... 58

CHAPTER SIX 61

6 RESULTS AND DESCUSSION....61

6.1 General.... 61
6.2 Model Results and Prototype.... 61

6.2.1 Results due to Self weight 61
6.2.2 Results due to Walkway load 63
6.3 Model Results and Experimental 66
6.3.1 Support Reactions 66
6.3.2 Deflections 67
6.3.3 Stresses 75

CHAPTER SEVEN 78

7 CONCLUSIONS AND RECOMMENDATIONS 78

7.1 Conclusions 78
7.2 Recommendations 79

REFERENCES 80

VITAE 82

LIST OF TABLES

Table 6.1 Reactions due to self weight for the model and prototype 61

Table 6.2 Deflections due to self weight for the model and prototype 62

Table 6.3 Stresses due to self weight for the model and prototype. 63

Table 6.4 Reactions due to walkway load for the model and prototype …….....64

Table 6.5 Deflections due to walkway load for the model and prototype.....64

Table 6.6 Stresses due to walkway load for the model and prototype..... 65

Table 6.7 Reactions due to Load Cases on the Slab Bridge 66

Table 6.8 Deflection due to fully loaded by sand of (1.20 kN/m^2) 68

Table 6.9 Deflection due to fully loaded by sand of (1.741 kN/m^2). 69

Table 6.10 Deflection due to Walkway when loaded by sand of (1.741 kN/m^2)..... 70

Table 6.11 Deflection due to Walkway Loads + Two trucks loads case 1 71

Table 6.12 Deflection due to Walkway Loads + Two trucks loads case 2.. 72

Table 6.13 Deflection due to Walkway Loads + Two trucks loads case 3.. 73

Table 6.14 Deflection due to Walkway Loads + Two trucks loads case 4.. 74

Table 6.15 Stresses due to fully loaded by sand of (1.20 kN/m^2) 75

Table 6.16 Stresses due to fully loaded by sand of (1.741 kN/m^2). 76

Table 6.17 Stresses due to Walkway when loaded by sand of (1.741 kN/m^2).. 76

Table 6.18 Stresses due to load case 1 76

Table 6.19 Stresses due to load case 2..... 77

Table 6.20 Stresses due to load case 3..... 77

Table 6.21 Stresses due to load case 4..... 77

LIST OF FIGURES

Figure 1.1 Details showing Al-Awali Bridge and the Road 4 highway 2
Figure 1.2 Plan of Part 4 and Part 3 2
Figure 1.3 Section of sidewalk on the Western edge 3
Figure 1.4 Plan showing dimensions and curvatures and Walkway of Part 4 3
Figure 1.5 Cracking at the bottom of the slab 4
Figure 1.6 Cracking at the bottom of the slab 4
Figure 1.7 High deflection at the Western edge 5

Figure 3.1 Location of bearings (Support) on the Abutment 19
Figure 3.2 Finite element mesh of the Part 4 of the slab bridge 20
Figure 3.3 Local and global axes 20
Figure 3.4 Self weight of the edge beam 21
Figure 3.5 Self-weight of the New Jersey barrier 22
Figure 3.6 Walkway slab weight 22
Figure 3.7 Asphalt weight 23
Figure 3.8 Live loads on walkway 24
Figure 3.9 Loading configuration of MOC truck 24
Figure 3.10 MOC Truck 25
Figure 3.11 Typical live load position on the deck (Truck Loads) 25
Figure 3.12 Locations of maximum deflection under dead load 26
Figure 3.13 Deflection shape of western edge under dead load 26
Figure 3.14 Deflection shape under dead load 27
Figure 3.15 Shear Stress (SQY) on the deck slab due to dead load 28
Figure 3.16 Moment Mx due to dead load (Tension bottom) 29
Figure 3.17 Moment My due to dead loads 30
Figure 3.18 Torsional moment Mxy due to dead load 31
Figure 3.19 Principal Stress at the bottom of the slab under dead load 32
Figure 3.20 Principal Stress contours under dead load 32

Figure 4.1 Actual and scaled loads **36**
Figure 4.2 Plan of part 4 skew slab **39**
Figure 4.3 Formwork of part 4 skew slab **39**
Figure 4.4 Top steel of part 4 skew slab **40**
Figure 4.5 Bottom steel of part 4 skew slab **40**
Figure 4.6 Longitudinal sections in part 4 skew slab **41**
Figure 4.7 Perpendicular sections in part 4 skew slab **42**
Figure 4.8 Steel bars inside the formwork **43**
Figure 4.9 Concrete casting of the model **44**
Figure 4.10 Slab model over the supports **45**
Figure 4.11 Load cell and rubber pad **47**
Figure 4.12 Two perpendicular directions strain gauge **47**
Figure 4.13 Linear voltage displacement transducers (LVDT) **48**
Figure 4.14 Portable data logger **48**
Figure 4.15 Strain gauges locations at the top and bottom **49**
Figure 4.16 LVDT's locations **49**
Figure 4.17 Carton boxes with sand inside at 6.6 cm **53**
Figure 4.18 Carton boxes with sand inside at 9.6 cm **54**
Figure 4.19 Walkway loads at 9.6 cm height with two trucks **54**
Figure 4.20 Walkway loads at 9.6 cm height with two trucks **55**
Figure 4.21 Walkway loads at 9.6 cm height with two trucks **55**
Figure 4.22 Walkway loads at 9.6 cm height with two trucks **55**

Figure 5.1 Location of bearings (Support) on the Abutment **57**
Figure 5.2 Finite element mesh of the Part 4 of the slab bridge **57**
Figure 5.3 Loading configuration of MOC truck (Truck Load) **59**
Figure 5.4 MOC truck (Truck Load) **59**
Figure 5.5 Top view of MOC Truck (Truck Load) **60**
Figure 5.6 Typical Live load Position on the Deck (Truck Load) **60**

Figure 6.1 Deck slab showing the support nodes..... 66
Figure 6.2 Location selected for deflection readings..... 67
Figure 6.3 Uniform load of sand of (1.20 kN/m^2). 68
Figure 6.4 Uniform load of sand of (1.741 kN/m^2). 69
Figure 6.5 Walkway Uniform load of sand of (1.741 kN/m^2). 70
Figure 6.6 Walkway Uniform load and Trucks loads case 1..... 71
Figure 6.7 Walkway Uniform load and Trucks loads case 2..... 72
Figure 6.8 Walkway Uniform load and Trucks loads case 3..... 73
Figure 6.9 Walkway Uniform load and Trucks loads case 4..... 74
Figure 6.10 Plates at which the stresses are selected..... 75

THESIS ABSTRACT

NAME: **FARHAT ABDUL-MUNIM ISAILI**

TITLE: **A MODEL–BASED STUDY OF A CURVED AND SKEWED SLAB TYPE BRIDGE DECK USED IN MAKKAH.**

DEPARTMENT: **CIVIL ENGINEERING**

DATE: **April, 2011**

Tight geometric requirements are often placed on highway structures due to right-of-way restrictions in congested urban areas. Skewed and/or horizontally curved bridges are among the some economical options for satisfying these demands. Increasingly strict and complex site constraints are leading to bridge projects with longer spans, more severe curvature and more complex geometries. These characteristics exacerbate the inherent three-dimensional (3D) response of curved and skewed bridge structures. As a result, the behavior of these types of bridges needs to be better understood. The model study can be utilized to understand the behavior and response of bridges. Such a study can also help in verifying the analytical results.

In this study, a scaled model of a skewed concrete slab type bridge deck was constructed in the laboratory. This slab model is simply supported on the same number of bearings as the prototype to get the same behavior; steel I-beams were used for this purpose. The Linear Variable Differential Transformer LVDTs sensors were placed at the bottom of the slab model to measure the deflection at several locations; also strain gages were installed at some key locations to record the strains. At critical bearing locations, load cells were used to record the reactions

because of loading. At loading time, visual observation was made for the slab deck behavior and response.

Two types of loading were used in this research; the first type is the superimposed dead loads, which were produced by using bags of sand. The second type of loading is the trucks or vehicles loads which were also produced by using small wooden boxes and sand bags.

The behavior of the skewed slab has been studied and discussed by comparing the experimental results with the finite element to observe the accuracy of the theoretical predictions.

MASTER OF SCIENCE DEGREE
KING FAHD UNIVERSITY OF PETROLEUM AND MINERALS
DHAHRAN - 31261, SAUDI ARABIA

ملخص الرسالة

الإســـــــــــم : فرحات عبد المنعم عسيلي

عنوان الرسالة : الدراسة النموذجيه لبلاطة الجسر الخرساني المنحي والمنحرف المستخدم في مكة المكرمة

التخصـــــص : الهندسة المدنية

تاريخ التـخرج : إبريل 2011م

غالبـاً مـا يـتم وضـع متطلبـات هندسـية مشـددة علـى هياكـل الطـرق السـريعة نظـراً للقيـود فـي المنـاطق الحضـرية المكتظـة . الجسـور المنحرفـه و/أو المنحنيـه أفقيـاً هـي مـن بعـض الخيـارات الاقتصـادية لتلبيـة هـذه الاحتياجـات .لكـن مـع زيـادة التعقيـد والقيـود فـي مواقـع العمـل فـان ذلـك يـؤدي الـى انشـاء جسـور ذات امتـداد أطـول وأكثـر شـدة فـي الانحنـاء بحيـث يصـبح شـكلها الهندسـي أكثـر تعقيـداً .هـذه الخصـائص تـؤدي إلـى تفـاقم وتعقيـد اسـتجابة هيـاكلال الجسـور ثالاثيـة الابعـاد ذات الانحنـاء والانحـراف . بنـاءً علـى مـا سـبق ذكـره، فـان سـلوك هـذه الأنـواع مـن الجسـور بحاجـة إلـى دراسـة وفهـم اكثـر تعمقـا، ودراسـة الآثـار المترتبـة مـن التحاليـل والتصـاميم التقديريـه والتقريبيـه المختلفـه علـى سـلامة المنشـأت. ويجـب الاخـذ بعـين الاعتبـار دراسـة وتوضـيح آليـة الانشـاء والاقتصـاد لهـذه الانـواع مـن الجسـور ذات الانحـراف والانحـاء. لـذلك فانـه مـن المكـن اسـتخدام الدراسـات النموذجيـة لفهـم سـلوك واسـتجابة هـذه الجسـور للاحمـال الواقعه. و يمكن أن تساعد هذه الدراسات أيضا في التحقق من النتائج التحليلية.

فـي هـذه الدراسـة، تـم بنـاء نمـوذج مصـغر الابعـاد لبلاطـة جسـر خرسـاني منحنـي ومنحـرف الشـكل فـي المختبـر .هـذا النمـوذج تـم روفعـه وتحميلـه علـى دعـائم وركـائز بـنفس عـدد الركـائز فـي الجسـر الخرسـاني الحقيقـي وذلـك للحصـول علـى نفـس السـلوك مـا بـين الجسـر الحقيقـي والنمـوذج المعـد للاختبـارات؛ وقـد تـم اسـتخدام ركـائز مـن الحديـد الصـلب ذو الشـكل (I) لهـذا الغـرض .وتـم وضـع أجهـزة استشـعار وحركـه افقيـه فـي الوجـه السـفلي لنمـوذج بلاطـة الجسـر المنحنـي فـي العديـد مـن المواقـع؛ كمـا تـم تركيـب اجهـزة قيـاس التمـدد فـي بعـض المواقـع الرئيسـية لتسـجيل قـراءات التمـدد اثنـاء عمليـة التحميـل ،وقـد تـم اسـتخدام خلايـا التحميـل لتسـجيل ردود الافعـال علـى الركـائز اثنـاء عمليـة التحميـل

التحميـل، وقـد تمـت مراقبـة بلاطـة الجسـر اثنـاء عمليـة التحميـل بصـريا لفهـم سـلوك البلاطـة مـع عمليـة التحميـل وملاحظة وجود التغيرات على البلاطه والدعائم.

وقـد تـم اسـتخدام نـوعين مـن الاحمـال فـي هـذه الدراسـة؛ النـوع الأول هـو الاحمـال الميتـه المركمـه، التـي تـم إجراؤهـا باسـتخدام أكيـاس الرمـل .النـوع الثـاني مـن التحميـل هـو أحمـال المركبـات التـي تـم اجراؤهـا أيضـا باسـتخدام صـناديق خشبية صغيرة واكياس الرمل.

وقـد تمـت دراسـة سـلوك هـذا النـوع مـن البلاطـات المنحيـة وتمـت مناقشـتها وذلـك بمقارنـة النتـائج التجريبيـة بالنتـائج التحليليه باستخدام الحاسوب لمراقبة مدى دقة التحاليل والحسابات النظرية.

درجة الماجستير في العلوم
جامعة الملك فهد للبترول والمعادن
الظهران - 31261
المملكة العربية السعودية

CHAPTER ONE

INTRODUCTION

1.1 General

The Al-Awali Bridge is located in the Al-awali District on the outskirt of Makkah on the North-East of the Haram Sharif at 21^{o}-36 ^{o}N latitude and 39.88 ^{o}E longitude. The Al-Awali road crosses the main eight (8) lane highway Road No.4 leading to Makkah

The road is a 2 lane road for traffic going to Al-Awali district which passes under the main highway Road No. 4. A single span bridge is provided on the highway for the road crossing.

As seen in Figures 1, the bridge is a single span bridge over the Al-Awali road and Road 4 highway with both roads having a curved profile at the intersection. The curved profiles results in a skewed single span bridge with a high angle of skew of about 63° and a bridge with complex geometry. It can be seen from Figures 1.1, that the width of Al-Awali underpass varies significantly with the width increasing substantially with the width increasing substantially towards the Western edge. The bridge deck consists of four structurally separated parts of simply-supported skewed slab. The Part 4, which has suffered extensive cracking and has noticeable sag.

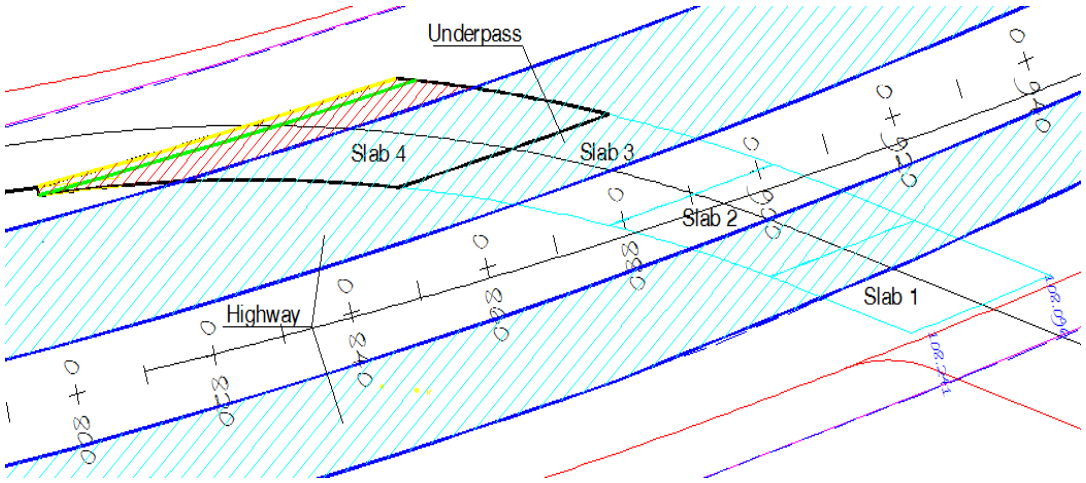

Figure 1.1 Details showing Al-Awali Bridge and the Road 4 highway.

A zoom in view of the Part 4 of the Al-Awali slab bridge is shown in Figure 1.2. The roadway and abutments of Part 4 have a radial profile as shown in the figure. The span of the Part 4 of the bridge in the direction of the roadway (skew direction) on the Eastern edge adjacent to the expansion joint of Part 3 is about 31.9m and it increases substantially to a width of about 52m at the outer Western edge. The NE and SW abutments have a significant curvature dictated by the highway geometry.

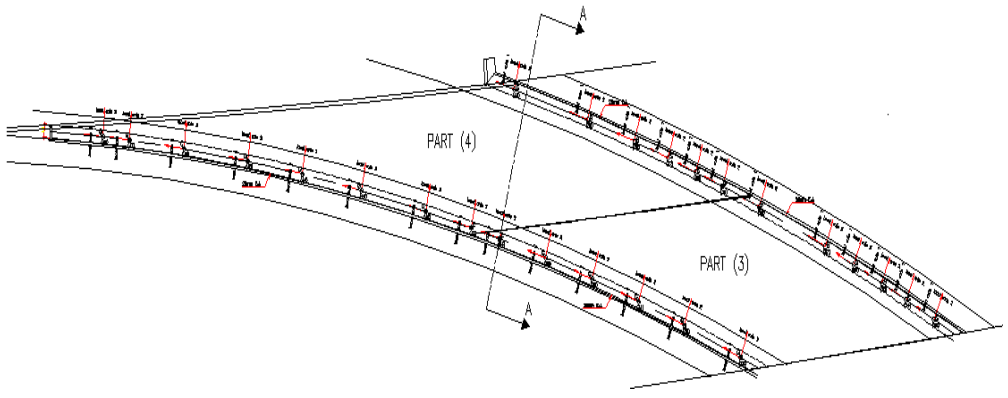

Figure 1.2 Plan of Part 4 and Part 3.

The cross section of the side walk at the Western edge of the bridge is shown in Figure 1.3. On the outer edge on Western side there is reinforced concrete beam which is cast integrally with RC deck slab. The total width of the walkway from the edge of the curb to the slab is about 4 m. A New Jersey barrier is placed at 3m from the road way and the sidewalks are 25 cm thick. The thickness of asphalt concrete on the road way is 5 cm. Figure 1.4 is a plan showing the dimension of walkways and the curvature of the abutment in the Part-4 of the bridge which has been studied.

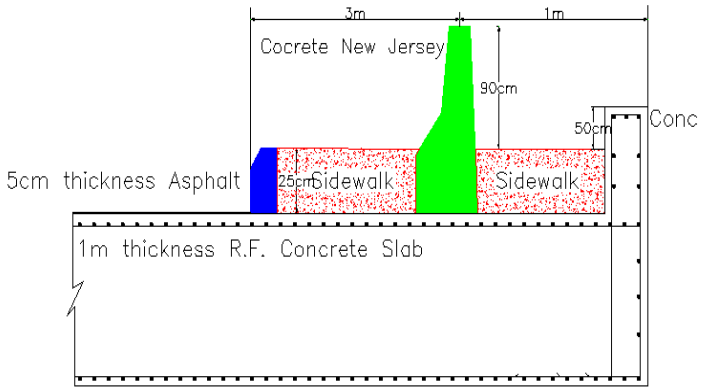

Figure 1.3 Section of sidewalk on the Western edge

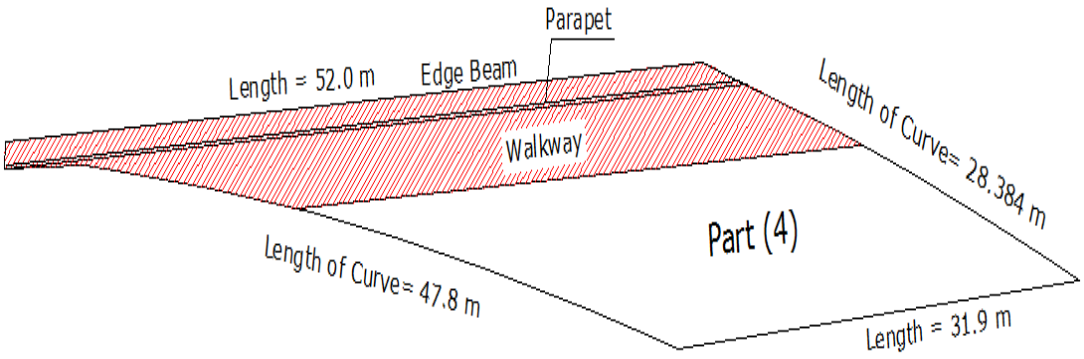

Figure 1.4 Plan showing dimensions and curvatures and Walkway of Part 4

The main problem in the bridge is that it showed substantial cracking on the bottom of the slab, and also on the vertical face of the slab on the N-W and S-E edge. Cracking in reinforced concrete structures is fairly typical, but the density and magnitude of the cracks on this particular bridge were considered to be excessive. Figures 1.5 and 1.6 show clearly a visible cracking at the bottom of the slab.

A thorough visual inspection revealed several problems related to structural condition and serviceability, much of the problems are attributable to the highly skewed geometry of the deck slab and the curving abutment that resulted in a very long span on the N-W and S-E longitudinal edge.

The second main problem is the deflection on the long Western edge of Part 4, which shows noticeable deflection. The maximum deflection occurs about 20 m from the NW corner of the slab. Figure 1.7 shows clearly visible large deflection at the Western edge.

Figure 1.5

Figure 1.6

Figures 1.5 and 1.6 Cracking at the bottom of the slab

Figure 1.7 High deflection at the Western edge

A study was constructed by a KFUPM team in which a linear FE model was used using STAAD pro. The limitation of this study was that the FE model was used on uncracked bridge deck. It is likely that significant cracking in conjunction with high skewed geometry, the actual behavior and response of the deck may be different.

It is of interest to study the actual behavior by understanding an experimental study of a scaled model of this bridge.

1.2 Needs for this Research

As mentioned above, the geometry of skew slab deck creates special characteristics, which will affect the response of the curved and skewed slab deck of the bridge. These type of slabs needs to be better understood to get the behavior and find the solutions to construct this type of structures away from problems of cracks and failure. In this

research, the behavior of the skewed slabs will be observed through model tests, and the experimental tests results will be compared with theoretical results to confirm the accuracy of the model tests. The theoretical tests will be performed by Finite Element Method (FEM) program, using STAAD pro. The experimental tests will be performed by constructing a scaled model of the skewed slab. The data will be compared to understand the behavior and observe the accuracy of the theoretical predictions.

1.3 Objectives and Scope of Research

1.3.1 Objectives

The objective of this study is to make a load testing by modeling and scaling the skew slab for part four of Al- Awali Bridge to obtain the experimental data and observation, which will then be verified by a finite element based analytical study of the model. This study will shade light on the behavior of the skew slab and the accuracy of the theoretical predictions.

The primary objectives of this work are:

1. Ascertain the degree of safety and serviceability of the bridge deck in Part 4 of Al-Awali Bridge by undertaking testing of a scaled model of the actual bridge.
2. Compare the accuracy of the theoretical predictions with the experimental data and observations made from testing the model.

1.3.2 Scope of Research

Only the scaled model of the part 4 of the bridge deck will be used in this study. This model will be used both in experimental and theoretical investigation using the material properties used in constructing the model. The live loads will consist of scaled down loading of AASHTO HS 20 truck loading for highway bridges.

1.4 Research Methodology

To accomplish the above objectives, this research will use a methodology comprising the following tasks.

Task 1: Literature Review.

A comprehensive literature review will be conducted in the areas related to the proposed research area. Curved and skewed slabs and scaled model slab bridges.

Task 2: Associated Problems and Past Studies of Al-Awali Bridge.

As mentioned earlier, a noticeable deflection of the longer longitudinal edge along North-West and South-East prompting a concern about the behaviour of the skewed deck slab. In addition to this deflection, cracks were observed at several places at the soffit of the deck slab, and also on the vertical face of the slab on the N-W and S-E edge.

In December (2008) and January (2009), Inspectech, a division of Kabbani Construction Group performed field instrumentation and live load testing.

In November (2009) and March (2010) Azad, Baluch, and Kalemu from KFUPM made a finite element analysis (FEM) testing model using STAAD.Pro program to analyze and study the behavior of Al- Awali bridge.

Task 3: Scale model of the bridge deck and fabrication

The model will be constructed by using a suitable scale factors which is factor of geometry, load factor, and strength factor to satisfactorily represent the actual bridge in a small scale. The model will be constructed using concrete and steel reinforcement so as to have the same material as the prototype. The model will be fabricated by contracting the work to an experienced contractor, who will be provided with specifications and instrumentation for casting.

Task 4: Experimental setup

The model will be simply supported on 6 support points along the short width and 8 support points along the longer width, representing the actual support system of the prototype bridge. Steel I-beam will be used to support the bearing pads. For the measurements of reactions, load cells will be used at some key support locations. LVTD's will be used at the underneath of the model at several locations to measure the deflection. Strain gages will be used at some selected locations to record strains.

Two types of loading will be used in this research:

1. Superimposed dead load, which will be made by using bags of sand.

2. Tracks or vehicles loads which will be made by using concrete blocks or sand bags.

The loads will be increased in small steps instrumentation until the impending failure of the slab is obtained.

Task 5: Experimental results

The resulting test data will be proposed in this study, recorded and analyzed.

The interpretation of the results will lead to a set of conclusions and recommendations.

Task 6: FE modeling and analysis of the model bridge

The present study is related to the Part 4 slab of the bridge in which shear and flexural cracks have been observed in the reinforced concrete deck slab. For analysis and design check of the Part 4 of the Al-Awali Bridge, a finite element model of the slab of the Part 4 of the existing bridge will be developed using Structural Analysis and Design Software STAAD Pro 2007.

Task 7: Discussion and Observation

The model will be observed during loading and testing, and the result compared to the theoretical will be discussed.

Task 8: Thesis Writing

The thesis will consist of six chapters; the first chapter will contain an introduction of the topic, the needs, and the scope of the research, the second chapter will contain the literature review related to the research subject.

Chapter number three will contain all details of the experiment work on the contrary of chapter four which will contain all details of the theoretical FE work. Then chapter five will contain the results and discussion of the work. And finally chapter six will include the conclusions.

CHAPTER TWO

LITERATURE REVIEW

Scaling and modeling is an important step towards effective management for testing the life loads applied to skew slabs. It is used to determine the operational characteristics and behavior of the systems such as stresses, moments, torsion, and cracks, etc.

William A. Litle (1966) established a reliable small scale ultimate strength modeling technique for wide-flange steel frameworks and presented the results of the first phase of his study. Five techniques have been considered for fabrication of small scale wide-flange steel beams. At the one-eighth to one-fifteenth scales envisioned for the model work, minimum thicknesses down to about 0.025-in would be required. Although the process produced reliable welds, test specimens showed occasional weld skips or incomplete welds due to imperfect alignment of the plates or due to "wandering" of the electron beam. These occurrences, coupled with the physical size limitations of existing vacuum chambers which house the electron beam equipment, caused rejection of this technique. Resistance welding of flange and web plates was also investigated. In order to establish proper techniques, a one- by two-bay three-story space framework was fabricated using one fifteenth scale 14*WF*103 members as columns and one fifteenth scale 21*WF*62 members as beams. He conclude that the mechanical properties and weld ability of SAE C1020 hot rolled steel permit its use as an ultimate strength model material for ASTM A36 steel structures, Milling wide-flange sections from hot rolled bar stock is a reliable and accurate process for fabricating small scale sections with element thicknesses down to 0.025-in, The machining process used to fabricate the wide flange

sections destroys the sharp break at the yield plateau but does not significantly influence the yield or ultimate strength, Tension and joint tests show that the Heliarc welding process (TIG) with Industrial Stainless 410 filler wires provides joints with more than adequate strength and ductility, Due to an unpredictable strength increase in the heat affected zones of non-annealed welded joints it is desirable to anneal whole frameworks before testing.

Corley et.al (1975) constructed and tested 1/10 scale micro-concrete model of new Potomac river crossing 1-266 at Washington D.C., Since the construction of this bridge would set several precedents, it was decided that structural model tests should be used to supplement the design calculations. The tests were carried out to study performance of the model bridge under application of dead load and design live load. In addition, behavior of the model under extreme overload was determined. The model was constructed of 3-ft.-long precast concrete segments that were sequentially grouted in position and post tensioned together. The use of precast segments was strictly for convenience in the laboratory. The results showed that, under the application of service load representing the dead load of the prototype and one live load plus impact under (HS 2044) loading, no structural cracking occurred and the model bridge remained essentially “elastic”.

Cheung (1978) studied analytically and experimentally the behavior of simply supported curved bridge decks with intermediate column supports. His analytical study was based on the finite-strip method, the results of which compared favorably with experimental values obtained from testing thirty 1:60 scale asbestos cement curved slab

decks. He conducted a static analysis of orthotropic curved bridge decks with two radial edges simply supported and the other two curved edges free, using a combination of Fourier series and the finite-difference technique. The governing fourth-order partial differential equation of orthotropic plates was converted to an ordinary differential equation and solved by the finite-difference method.

Harik and Pashanasangi (1985) presented a solution for the analysis of orthotropic curved decks subjected to uniform, partial uniform and patch loads, line and partial line loads in the radial and tangential directions, and point loads. The analysis is based upon an approach similar to that of the finite strip, but does not require the polynomial representation and minimization procedure often associated with the finite strip. The deck was divided into radially supported curved strips, whose deflections and loads were expressed in a Levy Fourier series. Convergence was achieved by increasing the number of modes instead of the number of elements.

Sato, Vecchio, and Andre (1987) tested the scale model to study the behavior of reinforced concrete elements. Two important aspects of model construction and response analysis are the requirements of geometric similitude and material similitude, both must be satisfied in order for a proper model to exist. Geometric similitude requires that all linear dimensions of both the specimen and the load application system be scaled down from the corresponding dimensions of a prototype by a constant ratio, $(1/S_1)$, where S_1 is the scale factor. Material similitude requires that, at any given load, the stress and strain in the model and prototype must be related by a constant stress factor S_s, and a constant strain factor S_e. The experimental results which they made indicate that reinforced

concrete scale models, when fabricated and tested to the requirements of replica scaling, can be used to accurately predict many aspects of prototype behavior under loading conditions.

Sritharan et.al (1999) tested five-story precast concrete building by PRESSS Precast Seismic Structural Systems) program, under simulated seismic loading. It was determined that, for seismic testing purposes, it would be only necessary to model 50 x 50 sq. ft plan area of the prototype buildings with 2 bays in each direction. The test building was then modeled at 60% scale of the resized prototype buildings in order to accommodate it inside the Charles Lee Powell Structural Laboratory at the University of California at San Diego (UCSD). This resulted in the test building having 30 x 30 sq. ft in plan, 7 ft 6 in. story height and 15 ft bay length and modeling all critical connections of a real building. They were expected that the different levels of pseudo dynamic testing together with stiffness measurement and inverse triangular tests, will sufficiently quantify the performance of the PRESSS building at different limit states.

McElwain and Laman (2000) gathered field response data from three in-service, curved, steel I-girder bridges to determine behavior when subjected to a test truck and normal truck traffic. Transverse bending distribution factors and dynamic load allowance were calculated from the data collected. Numerical grillage models of the three bridges were developed to determine if a simple numerical model will accurately predict actual field measured transverse bending distribution, deflections, and cross-frame and diaphragm shear forces. This study found that AASHTO specifications are conservative for both dynamic load allowance and transverse bending moment distribution. The

grillage models were found to predict with reasonable accuracy the behavior of a curved I-girder bridge. The instrumentation plan for each of the bridges was determined based on the location of the maximum positive bending moment in the instrumented span. Each bridge had a slightly different instrumentation configuration due to the geometry of the structure; however, the location of instruments on each bridge was based on the following criteria: (1) Strain gauges attached to the girder bottom flanges were located within 1 m of the maximum positive bending moment; (2) strain gauges attached to the girder bottom flanges were located away from girder splices and cross frames; (3) both flange tips of each girder were instrumented; (4) the cross frames or diaphragms nearest the maximum positive moment were instrumented; and (5) deflection measurements were taken near the location of the maximum positive bending moment. They found that agreement between grillage models and experimental measurements is good. The majority of the maximum grillage bending GDFs for all bridges did not deviate from the experimentally derived GDFs by >20% and were typically within 10%. It is recommended that the grillage model be used to predict the transverse load distribution in curved girder bridges.

Doulahl and Kabir (2001) adopted a non-linear finite element method using layered concept across the thickness to study its suitability for the analysis of reinforced concrete slabs with special emphasis on skew slabs. Only material nonlinearity has been considered here. An eight-nodded isoperimetric Mindlin plate element based on layering technique is used to account for transverse shear deformations. The layered technique is adopted in order to allow for the progressive development of cracks through the thickness at different sampling points. The non-linear effects due to cracking and crushing of

concrete and yielding of steel reinforcement are included. The material model behavior is based on the experimental observation reported by various authors. Rectangular and especially some reinforced concrete skew slabs have been picked up as examples to demonstrate the applicability and efficiency of the method. The analysis and design of reinforced concrete skew slabs are normally based on the linear elastic theories and limited up to yield load only. This work is an attempt towards that end to correlate the experimental behavior of few skew and rectangular slabs with the numerical predictions using simple and popularly accepted material models. They conclude that comparison of the numerical predictions with the experimental results demonstrates that the layering technique may suitably be employed for analyzing reinforced concrete slabs including skew ones. Comparing the numerical load-deflection curves with the experimental, it may be concluded that the model is able to predict the entire sequence fairly well under monotonically increasing transverse load for reinforced concrete skew slabs. The material models adopted for layered concrete and steel reinforcement are simple and may be adopted for numerical analysis of reinforced concrete skew slabs.

Miah and Kabir (2005) studied the behavior on reinforced concrete skew slab. They tested six skewed slab of concrete in the laboratory where the entire tested slab scaled to 1/6 model of prototype skew slabs, with using the same steel arrangement for all. The experimental observations were limited to measurement of deflection at different nodal points, concrete fiber strains at some top and bottom points of the slabs, steel strains, cracking patterns and observing the cracking and ultimate loads.

They observed that the load carrying capacity of skew slabs significantly depends on the skew angle. As can be expected, with the increase in skew angle stiffness of slab decrease and so is load carrying capacity.

Maher Shaker Qaqish (2006) studied the effect of skew angles distribution of bending moment in bridge slabs. He subjected 1.8 AASHTO truck loading, 1.8 AASHTO equivalent distributed loading and abnormal loading to the structural model. He compared the results for transverse and longitudinal moments with the results obtained from AASHTO specifications. This comparison shows that applying AASHTO specification for slab bridge deck is safe and economical.

Fam, Huitema and Meyer (2006) designed a highly curved concrete ramp bridge, which presented a challenge to bridge engineers due to the problems imposed by the complex environmental and geometric constraints. They maintain the stability of the structure by balancing the dead, pre-stressing and live loads with the reactive forces at supports which is of particular important. They proved that these bridges could be designed and constructed economically. By respecting the geometry of the curved road and the constraints of the underlying elements, these bridges provided both functionality as well as balance of visual elements.

Ozgur and White (2008) studied the behavior and design of horizontally curved and skewed I-girder bridges predicted by 3D FEA and 3D Grid models. They observed that major-axes of bending stresses and deflection are not affected significantly by the

geometric nonlinearity whereas the influence of geometric nonlinearity is noticeably high for the flange lateral bending stresses and radial deflections.

Research work has been done to model a structure, and for testing the behavior of skewed slabs. December (2008) and January (2009) Field instrumentation and live load testing were performed in by Inspectech, a division of Kabbani Construction Group to predict the behavior of Al- Awali bridge. November (2009) and March (2010) Azad, Baluch, and Kalemu from KFUPM made a finite element analysis (FEM) testing model using STAAD.Pro program to analyze and study the behavior of Al- Awali bridge.

CHAPTER THREE

THEORETICAL STUDY OF ACTUAL BRIDGE

3.1 Modeling of the Bridge Deck

The present study is related to the Part 4 slab of the bridge in which shear and flexural cracks have been observed in the reinforced concrete deck slab. For analysis and design check of the Part 4 of the Al-Awali Bridge, a finite element model of the slab of the Part 4 of the existing bridge was developed using Structural Analysis and Design Software STAAD Pro 2007.

The Part 4 of the slab bridge is supported on six pot bearings spaced at varying distances on the North-East abutment and eight pot bearings on the South-West abutment as shown in the Figure 3.1.

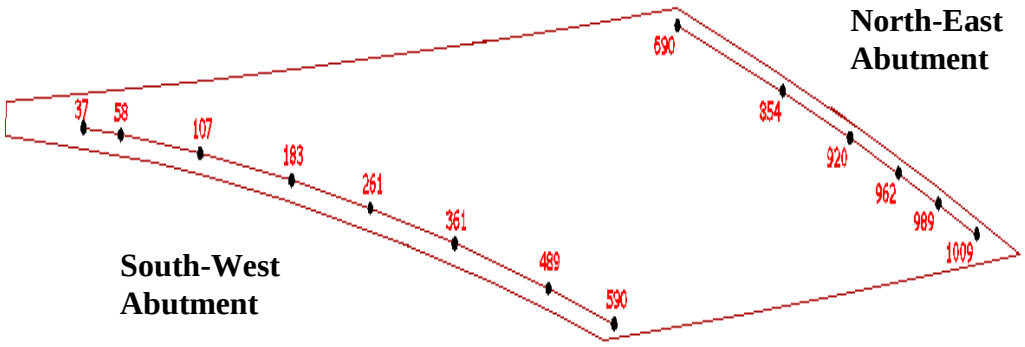

Figure 3.1. Location of bearings (Support) on the Abutment

The finite element model of the slab is shown in Figure 3.2. .The finite element mesh is 0.8m x 0.8m in size. The aspect ratio of the elements is 1 or less. The lines parallel to the roadway in the mesh indicates the boundary of the walkway and the barrier line. These lines have been placed to apply the barrier loads and the walkway loads on the slab. The finite element model comprises 760 elements and 2050 nodes. Plate elements are used for modeling the slab and the thickness of the plate is assigned as 1 meter. The global and local axis of a portion of the structure and the elements are shown in Figure 3.3.

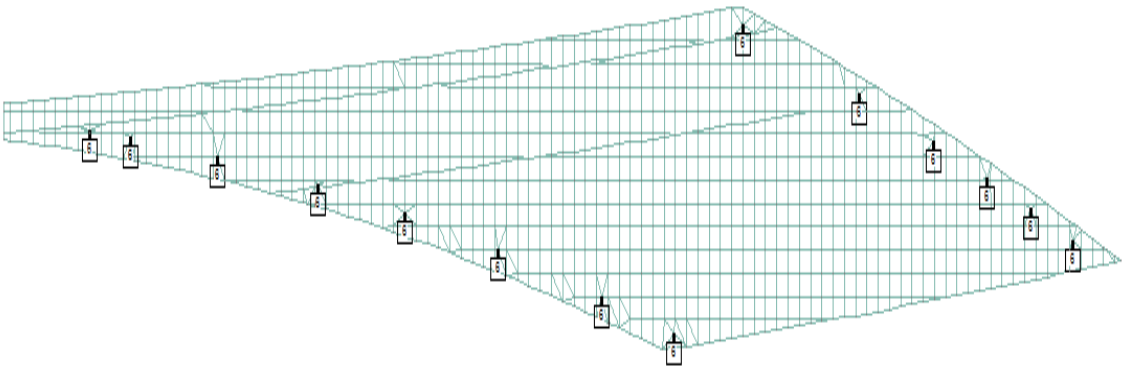

Figure 3.2 Finite element mesh of the Part 4 of the slab bridge

Figure 3.3 Local and global axes

3.2 Loads on the Slab Deck

The bridge deck slab will be analyzed for the following loads.

3.2.1 Dead Load

- Self weight of 1.0 m thick reinforced concrete slab
- Self weight of 0.3 x 1.75 m edge beam (Figure 3.4)
- New Jersey barrier weight = 0.31 m^2 x 24 = 7.68 kN/m (Figure 3.5)
- Weight of the walkway slab = 24 kN/m^3 x 0.25 = 6 kN/m^2 (Figure 3.6)
- Asphalt weight = 19 kN/m^3 x 0.05 = 0.95 kN/m^2 = 1 kN/m^2 (Figure 3.7)
- Live load on walkway = 5.2 kN/m^2 (Figure 3.8)

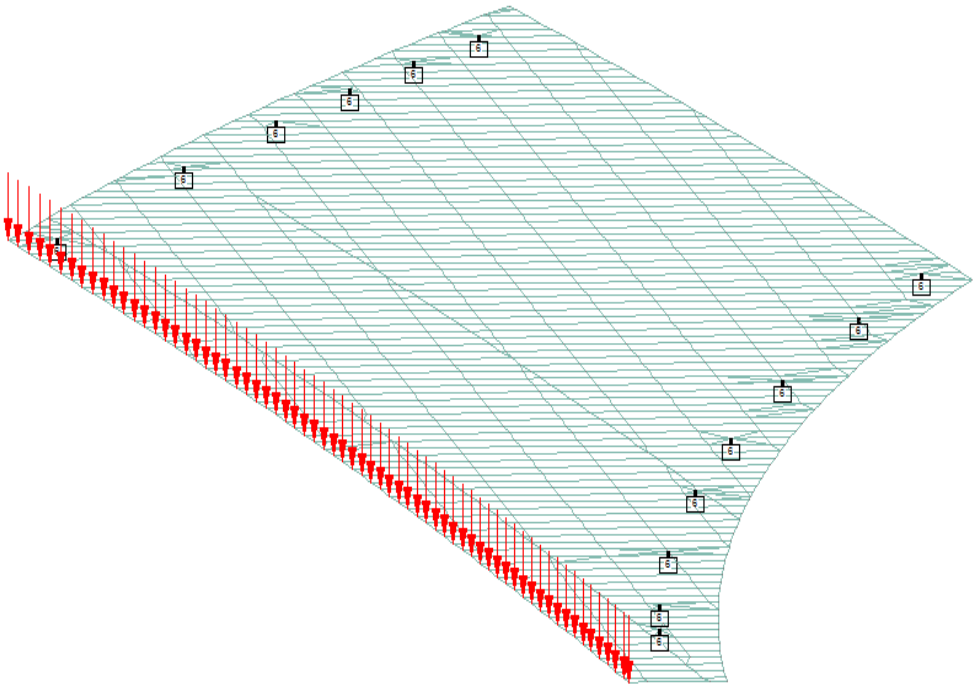

Figure 3.4 Self weight of the edge beam

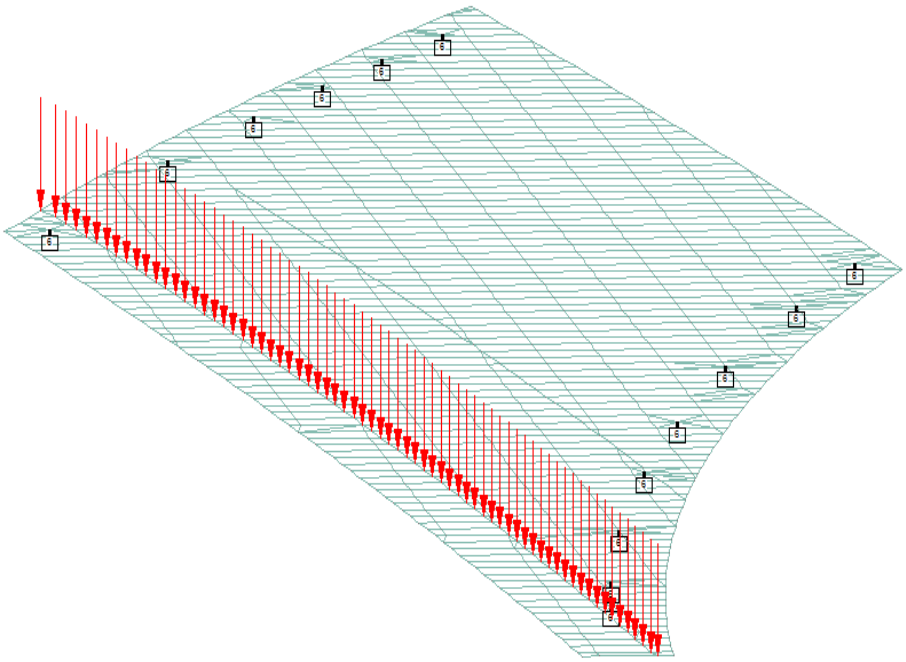

Figure 3.5 Self-weight of the New Jersey barrier

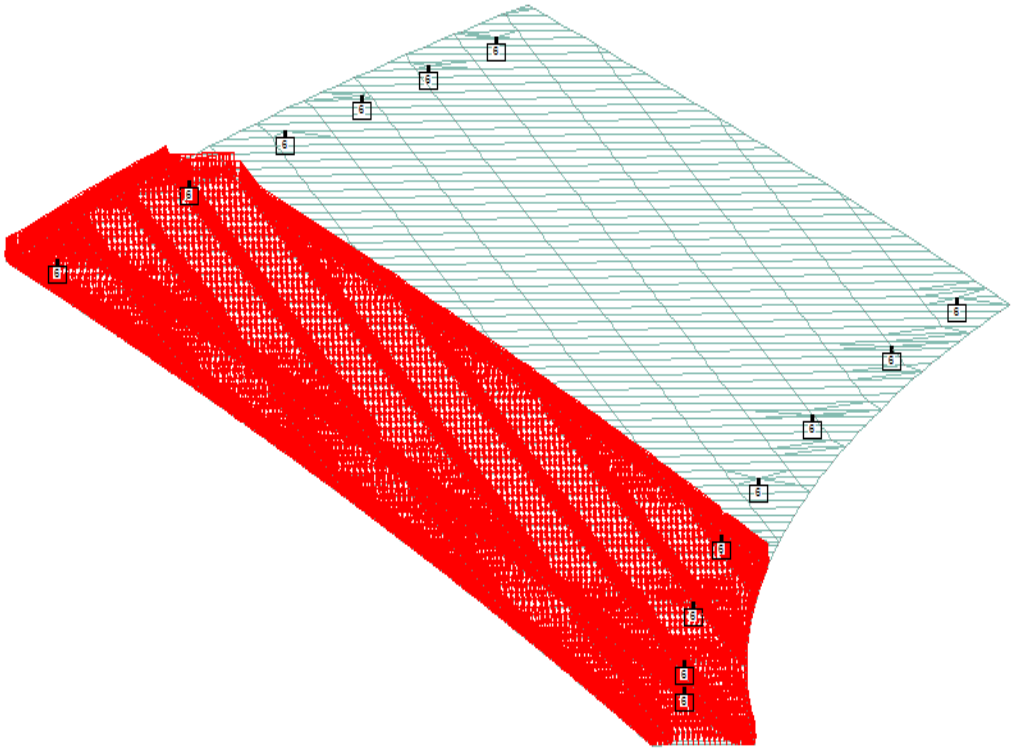

Figure 3.6 Walkway slab weight

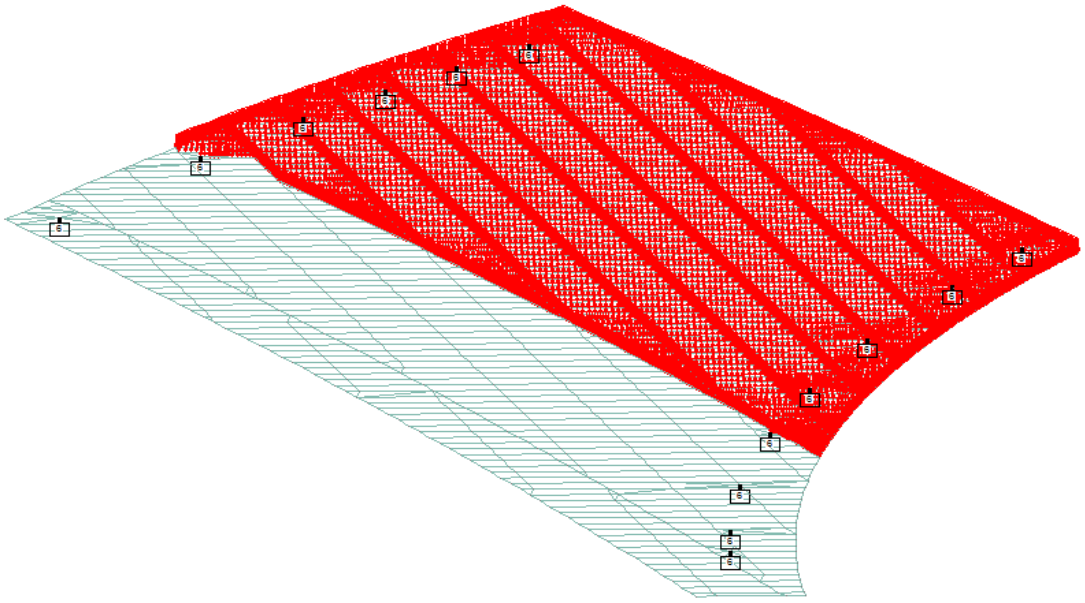

Figure 3.7 Asphalt weight

3.2.2 Live Loads

A walkway live load of 5.2 kN/m^2 is considered for the analysis of the deck slab as shown in Figure 3.8. The truck load considered in the design is the standard truck as per Ministry of Communication, Saudi Arabia recommendations. An impact factor of 30% is considered. The live load for the MOC truck consists of a leading load of 40 kN wheel followed by two loads at 4.3 m spacing with a value of 160 kN/wheel. The concentrated truck loads is shown in Figure 3.9 and the MOC truck is shown in Figure 3.10.The live load can be placed on any location of the deck slab and various live load cases were countered. A typical live load position of the trucks is shown in Figure 3.11.

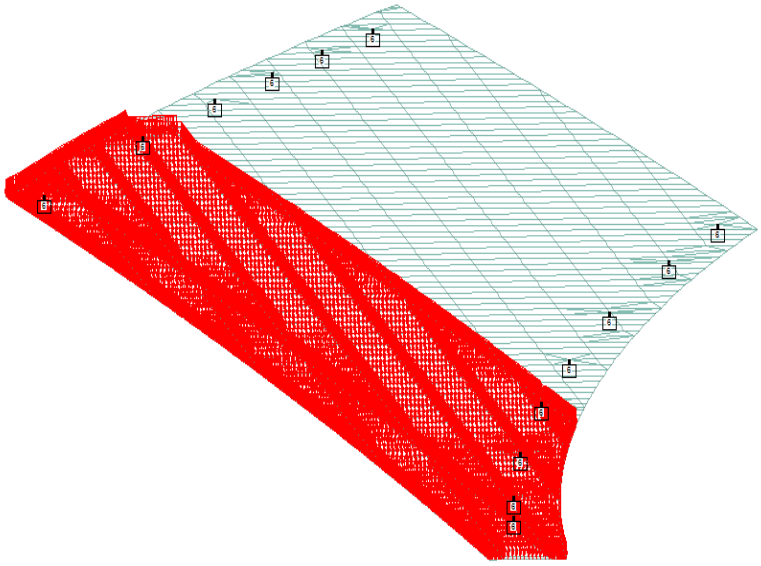

Figure 3.8 Live loads on walkway

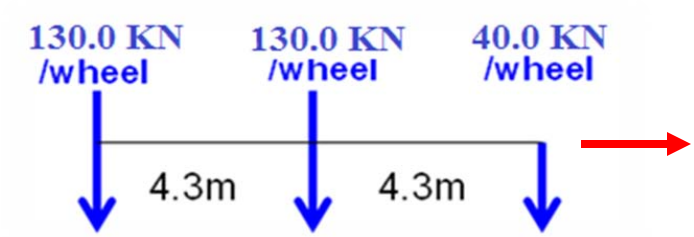

Figure 3.9 Loading configuration of MOC truck

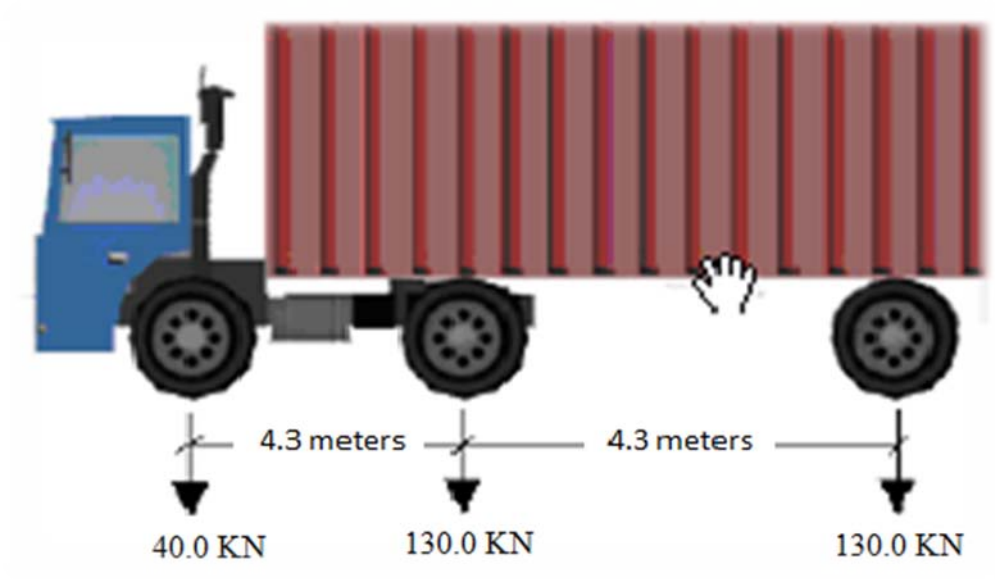

Figure 3.10 MOC Truck

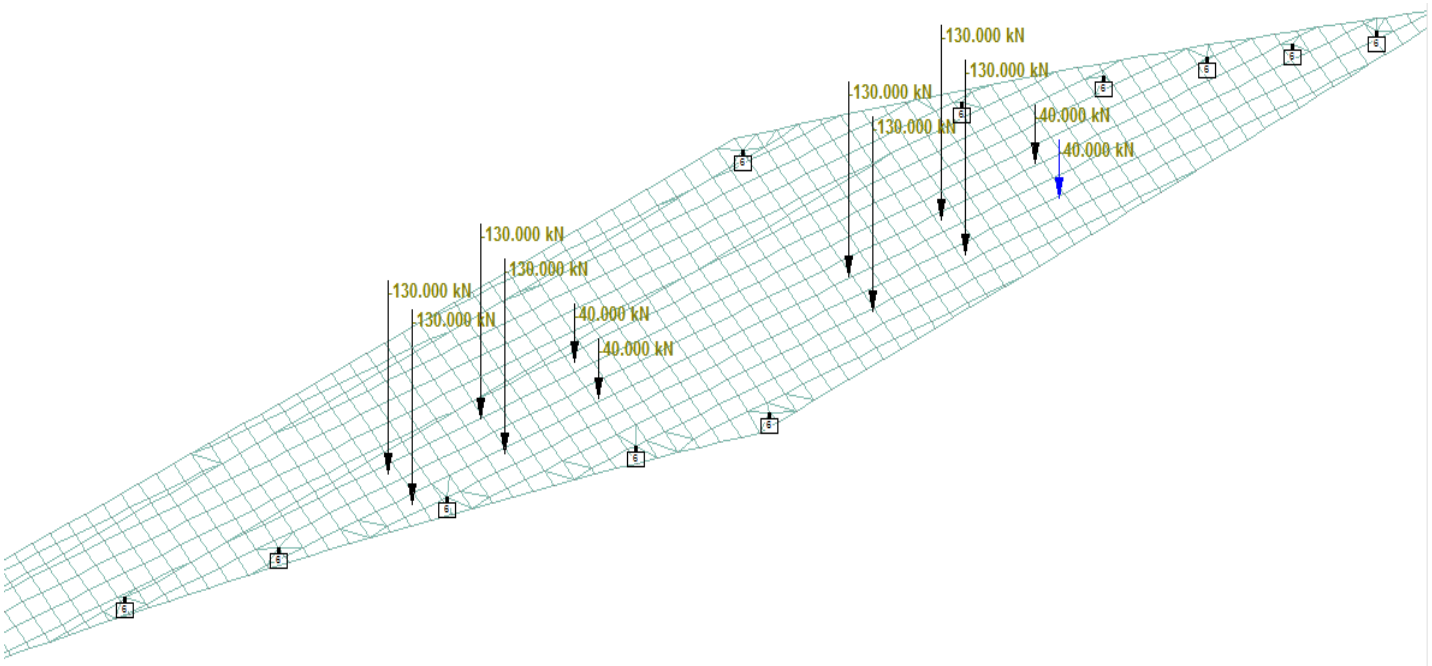

Figure 3.11 Typical live load position on the deck (Trucks Loads)

3.3 Maximum Deflection in the Slab Deck

The maximum defection of the long edge under dead load is about 189 mm. This deflection at the Western edge towards the NE abutment is clearly evident in the bridge at the site. The deflection is considered as high. It however occurs in a zone which has side walk 4m wide on the main highway and does not affect the serviceability of the traffic on the bridge. Figure 3.12 shows the nodes at which the deflection is the maximum and Figures 3.13 and 3.14 shows the deflection shape.

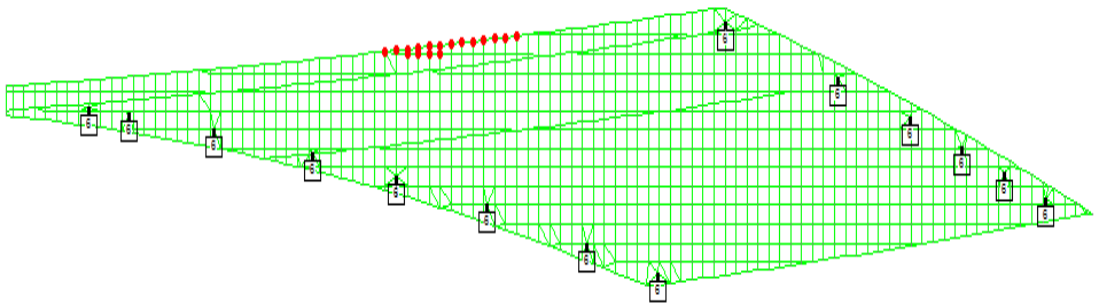

Figure 3.12 Locations of maximum deflection under dead load

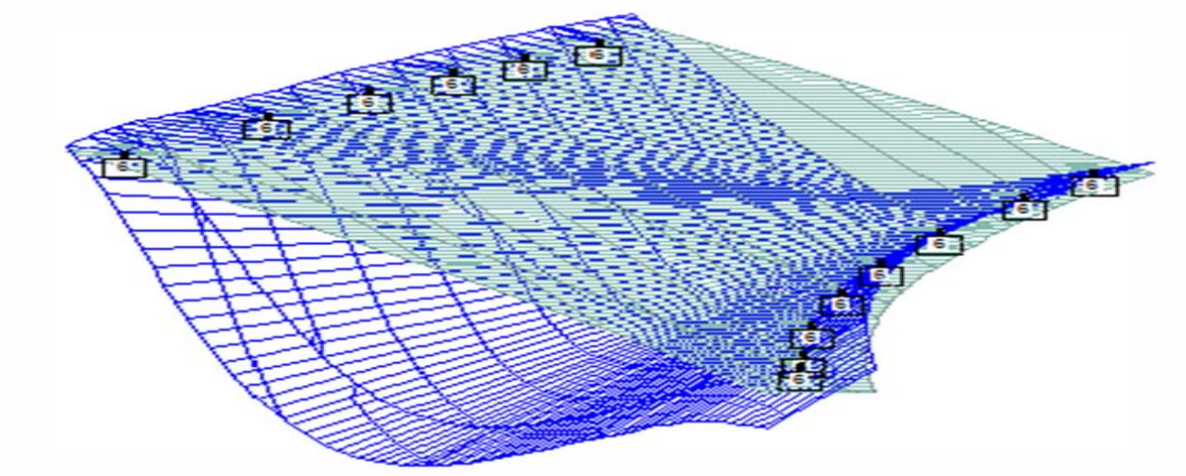

Figure 3.13 Deflection shape of western edge under dead load

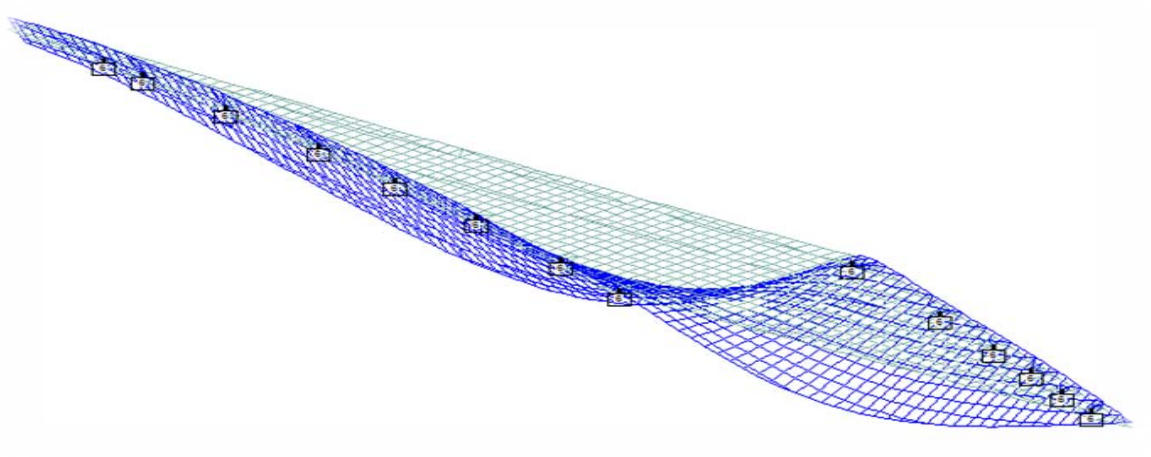

Figure 3.14 Deflection shape under dead load

3.4 Shear Stresses in the Slab Deck

The plot of vertical shear stress in the deck slab (SQY) is shown in Figure 3.15 due to dead loads. It can be seen that very high shear stress of about 2.25 MPa and an average shear stress of about 2 MPa occurs on the free long edge of the deck slab on the Western end of the underpass. This high shear zone is limited to narrow band adjacent to high reaction node on the NE abutment. A large number of fine diagonal shear cracks extending from bottom of the slab to the bottom of the edge beam can be seen on the Western edge of the slab at the site. It can be seen that localized high shear stress also exists on the Eastern edge at the expansion joint. The magnitude of shear sterss in this zone is however lower compared to the longer edge but may lead to some shear cracks which cannot be seen. Localized shear stresses also exist at the supports on the SW abutment as seen in Figure 3.15.

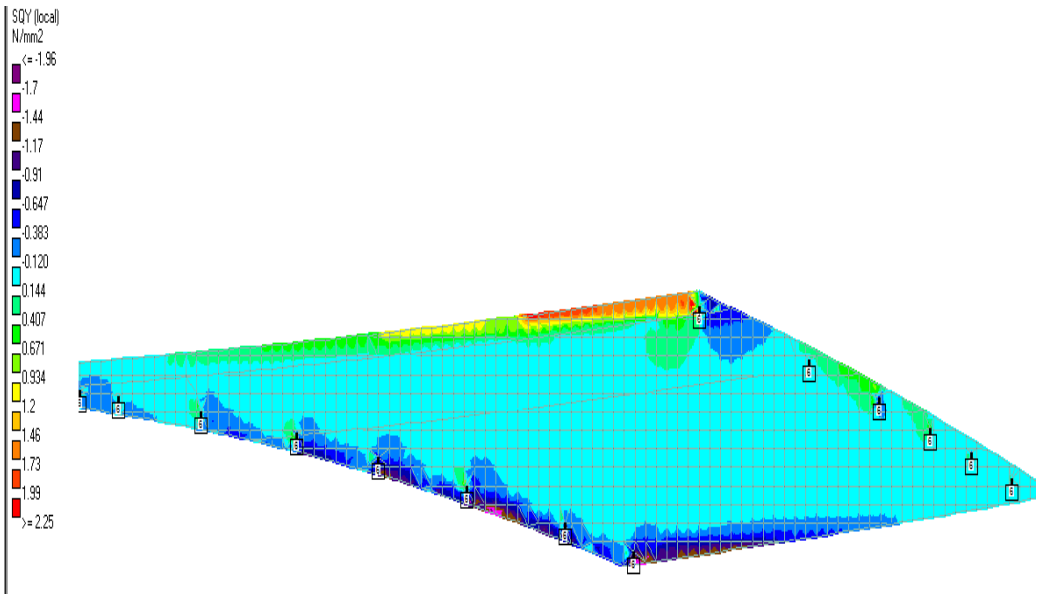

Figure 3.15 Shear Stress (SQY) on the deck slab due to dead load

3.5 Bending Moment Mx

The variation of moment Mx, in the slab is shown in Figure 3.16 due to dead loads. The moment Mx is maximum symmetrically about the line connecting the NW and SW corners of the slab. It can be inferred from the figure the main load transfer occurs along this path which results in very high reactions on the NW corner. The moment Mx at selected modes in this zone causes tension at the bottom of the slab and very high tension at the top of the slab occurs in a very limited zone near the NW high reaction corner as shown in Figure 3.16. The maximum moment Mx is 1968 kN-m/m. Tension at top due moment Mx in the range of 168 to 495 kN-m/m also occurs in areas adjacent to the supports on the NE and the SW abutments (see Figure 3.16).

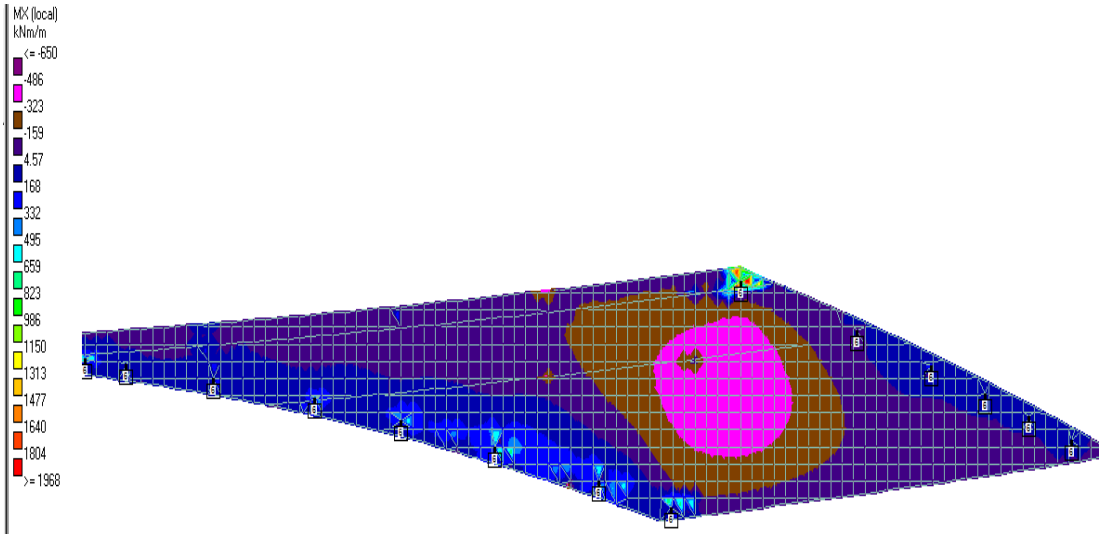

Figure 3.16 Moment Mx due to dead load (Tension bottom)

3.6 Bending Moment My

The variation of moment My, in the slab is shown in Figure 3.17due to dead loads. The moment My causing tension at the top of the slab in the zone extending from the NW to the SE corners of the slab. In zone adjacent to the NW corner of the slab emanating from the node # 690 with very high reaction the moment is very high and decreasing as one move towards the SE corner of the slab. The moment My at selected modes in this zone causes tension at the top of the slab. The moment is in the range 842 to 1853 kN-m/m. Moment My also causes high tension at the top of the slab. It occurs in a region extending from the Western edge of the slab where slab has a large deflection to the support on the SW abutment as shown in Figure 3.17. The maximum moment is 688 kN-m/m at the Western edge and a large zone shown in pink has an average moment of about 450 kN-m/m. (see Figure 3.17).

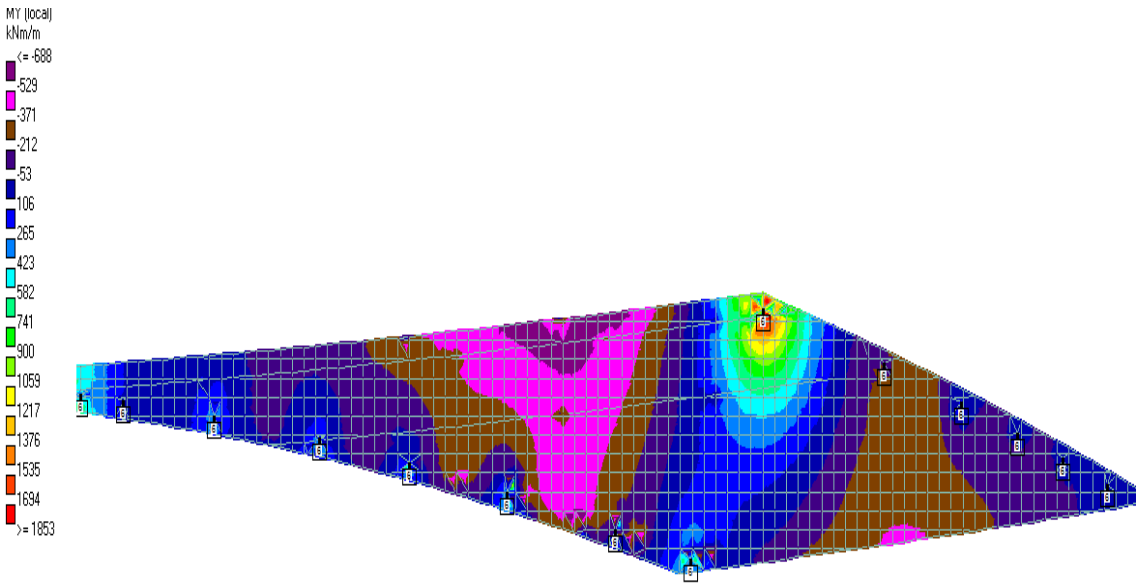

Figure 3.17 Moment My due to dead loads

3.7 Torsional Moment Mxy

Due to complex geometry and highly skewed nature of the bridge the dead load also results in a high torsional moment in the slab. The high torsional moments occurs in a band extending on both sides of the line joining the NW and SE supports. The variation of torsional moment Mxy, in the slab is shown in Figure 3.18. The maximum dead load torsional moment in the range of 1000 to 1145 kN-m/m occurs in zone near the Western edge as shown in Figure 3.18. The torsional moment decreases towards the SE corner with an average value of about 500 kN-m/m

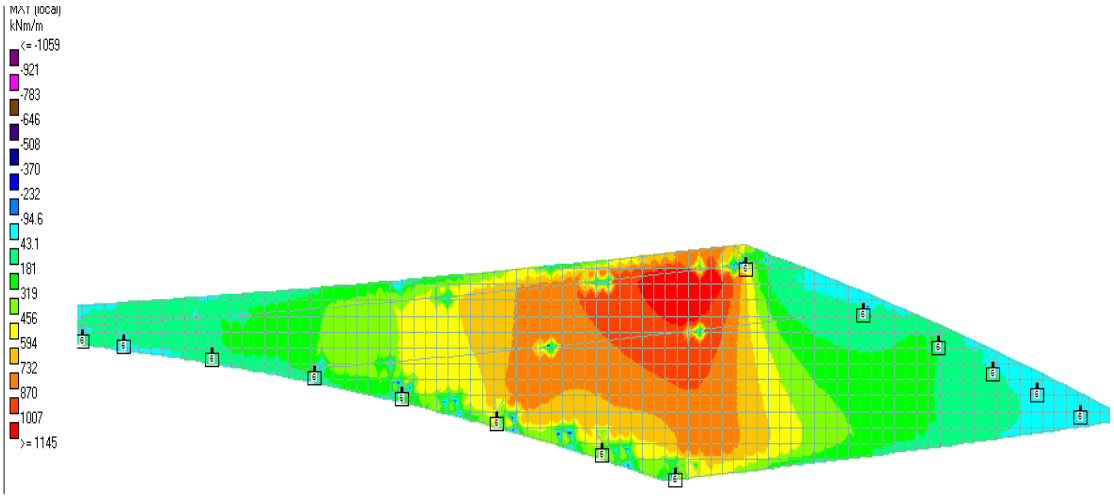

Figure 3.18 Torsional moment Mxy due to dead load

3.8 Principal Stress

Due to complex geometry and highly skewed nature of the bridge the tension at the bottom of the slab occurs due to the moments Mx, My and Mxy under the dead load. The principal moments and the associated principal stresses therefore are of high importance in predicting the cracking in the slab. The variation principal stresses in the deck slab at the bottom of the slab are shown in Figure 3.19 and the principal stress contours are shown in Figure 3.20. It can be seen that maximum principal stress occurs in the areas adjacent to the heavy concentrated reaction at the NW support. Principal stress of about 12.5 MPa occurs near the support. Along a line extending from the NW corner to the middle of the Western edge of the slab and a zone extending from this line towards the SE corner zone, the principal stresses are high and ranges from 5 MPa to 9 MPa (Figure 3.19). Cracking in this zone due to the principal tensile stress is visible in the slab.

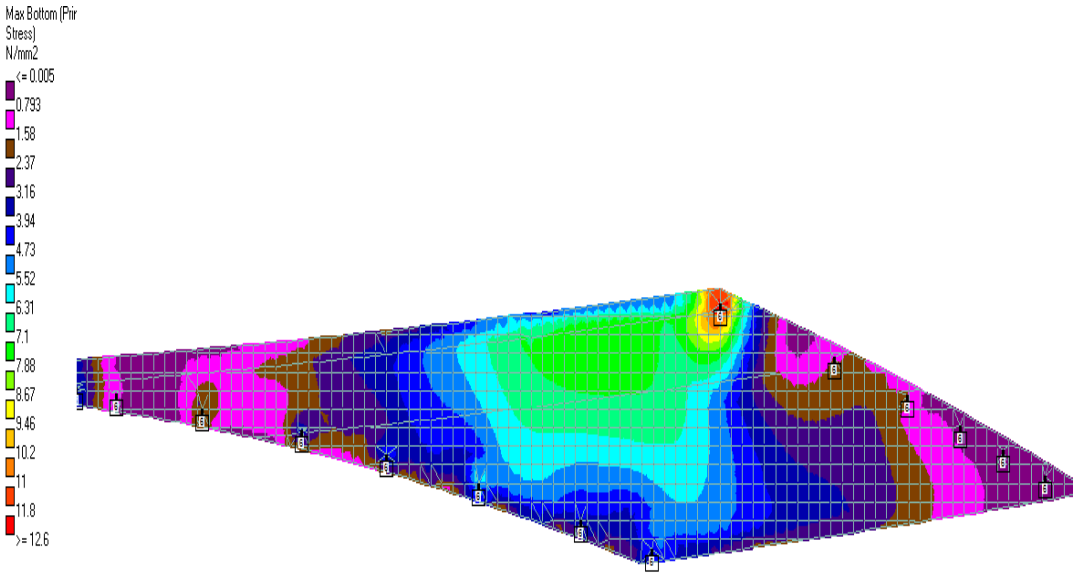

Figure 3.19 Principal Stress at the bottom of the slab under dead load

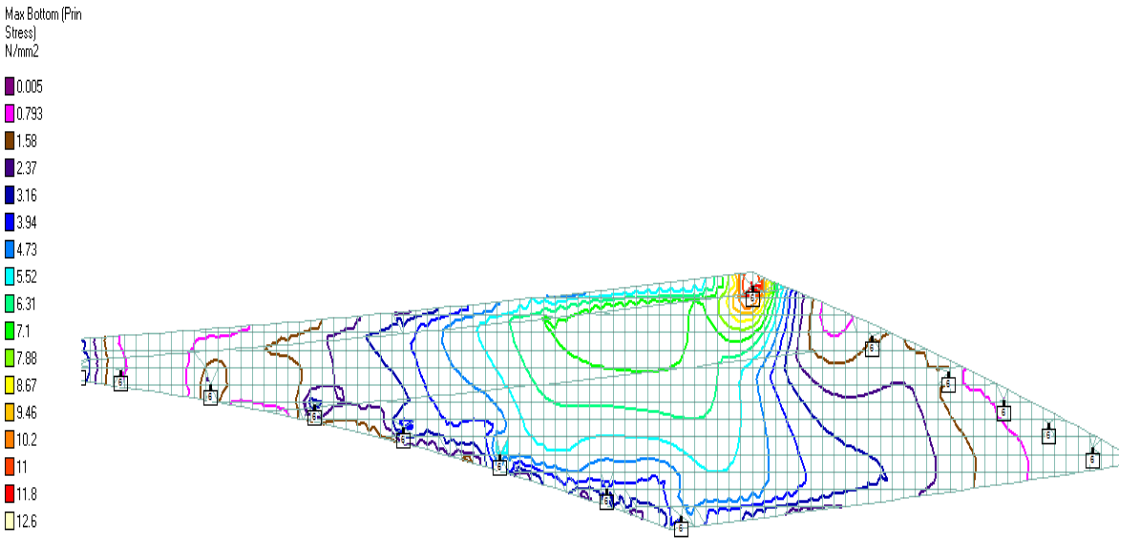

Figure 3.20 Principal Stress contours under dead load

3.9 Observations

Due to complex geometry and highly skewed nature of the bridge, the model shows many observations when analyzing by FEM, are as follows.

- Many Cracks were occurred on the free long edge span of the deck slab on the Western end of the underpass and on the abutment
- Cracking (flexural) was observed near the node which has maximum reaction in zone adjacent to the NW corner of the slab.
- Punching area on the node of maximum reaction adjacent to the NW corner of the slab.

CHAPTER FOUR

DETAILS OF THE EXPERIMENTAL

4.1 General

In this chapter, a brief introduction to analysis of 1/10 scaled skew slab deck is given.

The tests were carried out to study performance of the model slab under application of dead load and scaled live load of AASHTO HS 20 truck loading for highway bridges.

4.2 Choice of Scale

A linear scale of 1/10 was chosen for the bridge taken into consideration of: available space for testing, handling and cost. This scale represented a physical structure that was considered as not too small to use as representation model of the actual structure.

4.3 Dead Load Factor

The scaled factors for the dead loads were calculated depending on the scaled dimensions of the scaled model as following;

- Self weight of 1m reinforced concrete slab thickness has been scaled 1/10 to be 0.1m thickness.
- Self weight of 0.3 m x 1.75 m edge beam has been scaled to 1/1000.

The scale was proved as following;

By using the actual dimensions,

0.3 x 1.75 = 0.525 m^2

0.525 m^2 x 25 kN/m^3 = 13.125 KN/m

The length of the edge beam = 52.3 m

13.125 kN/m x 52.3 m = 686.44 kN

But when using the scaled dimensions,

0.03 x 0.175 = 0.00525 m^2

0.00525 m^2 x 25 kN/m^3 = 0.13125 kN/m

The scaled length of the edge beam = 5.23 m

0.13125 kN/m x 5.23 m = 0.68644 kN

Then the factor = 0.68644 kN/ 686.44 kN = 0.001 = 1/1000

So, the edge beam scaled factor is 1/1000

- New Jersey barrier weight = 0.31 m^2 has been scaled to 1/1000.

The same prove used as before.

Actual load = 0.31 m^2 x 25 KN/m^3 = 7.75 KN/m

Scaled load = 7.75 KN/m / 1000 = 0.0775 KN/m

0.0775 KN/m x 4.40 m = 0.341 KN

So, the New Jersey barrier scaled factor is 1/1000

- Weight of the walkway dead loads = 25 KN/m^3 x 0.25 m = 6.0 KN/m^2 has been scaled to 1/10, which is equal 0.60 KN/m^2.
- Live load on walkway = 5.2 KN/m^2 has been scaled to 1/10, which is equal 0.52 KN/m^2.

4.4 Live Load Factor

The slab deck has been analyzed for the live loads which have been scaled as follows.

Figure 3.1 shows a simply supported beam of a span L and L’ for a model with 1/10 scale where (L’ = L/10). The width of the beam is B and B’ where (B’ = B/10) and thickness is t and t’ where (t’ = t/10), using 1/10 linear scale for the model.

By using the original and scaled loads seen in Figure 4.1, the live loads scale factor was determined by considering magnitude of bending stress for the model as 1/10 that of the actual beam.

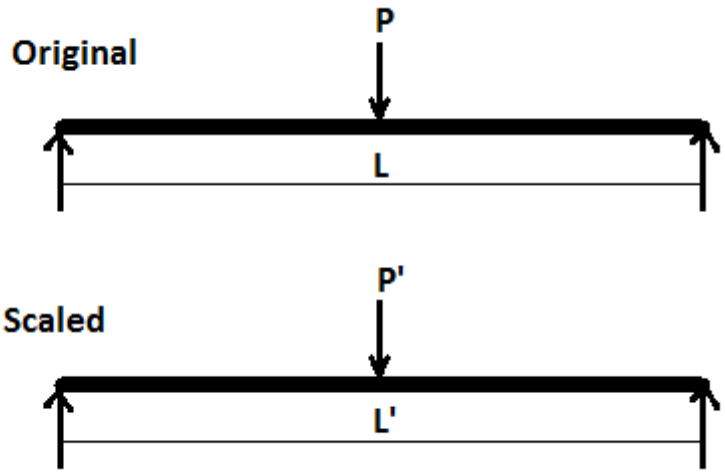

Figure 4.1 Actual and scaled loads

The maximum moment in the model is

$$m_{(model)} = \frac{P'L'}{4} \tag{3.1}$$

The maximum bending stress in the model f is given as

$$f_{(model)} = \frac{m_{(model)}}{S} \tag{3.2}$$

$$\text{Where S is elastic section modulus} = \frac{B' t'^2}{6}$$

$$f_{(model)} = \frac{P'L'}{4*\frac{1}{6}*B'(t')^2} = \frac{1.5\ P'L'}{B'(t')^2} \tag{3.3}$$

From Eq. (3.3),

$$f_{(model)} = 1.5\ P'*(\frac{L}{10})*\frac{1}{\frac{B}{10}*\frac{t^2}{10^2}}$$

$$f_{(model)} = \frac{150\ P'\ L}{B\ t^2} \tag{3.4}$$

For the original beam,

$$f_{(original)} = \frac{P\,L}{4*\frac{1}{6}*B(t)^2} = \frac{1.5\ P\,L}{B\ t^2} \tag{3.5}$$

Keeping stress scale 1/10,

$$f_{(model)} = \frac{f_{(original)}}{10}$$

$$\frac{150\ P'\ L}{B\ t^2} = \frac{1.5\ P\,L}{10\ B\ t^2} \tag{3.6}$$

$$From\ which \quad P' = (\frac{p}{1000}) \tag{3.75}$$

Then, the live load scaled factor is 1/1000

4.5 Model Fabrication

4.5.1 Formwork

The plan of part 4 skewed slab has been prepared to a scaled of 1:10. The plan view of the slab is shown in Figure 4.2, with the help of the carpenters in the maintenance department the formwork was prepared. The formwork has been transported to a subcontractor outside the University for reinforcement steel work. Formwork is shown in figure 4.3.

4.5.2 Steel Work

The amount of steel reinforcement for the model was down by a factor of one-tenth. The details of scaling down the steel of part 4 are as following.

Top steel:

1- For φ32 @ 133 mm in actual design:

Φ32 steel is equal # 10 steel with As = 1.25 in^2 and d = 1.26 in.

Number of bars in (1m) = 1000 mm/133 mm = 7.52 bars

$As = 7.52 * As_{(\varphi 32)}$

As = 7.52 * 1.25 in^2 = 9.40 in^2

Now the model steel area $As_{(m)}$ = As/ scale factor

$As_{(m)}$ = 9.40 in^2/10 = 0.94 in^2

By using bars #3 which have an area = 0.12 in^2

Number of bars = 0.94 in^2/0.12 in^2 = 7.833 bars

The spacing between bars S = 1000 mm/7.833 = 127 mm

Then use steel of #3 @ 110 mm in the model

2- For φ28 @ 166 mm in real design.

Use steel of #3 @ 200 mm in the model

Bottom steel:

1- For φ32 @ 266 mm in actual design.

Use steel of #4 @ 200 mm in the model

The steel details are shown in Figures 4.4, 4.5, 4.6 and 4.7 for top, bottom plans and sections.

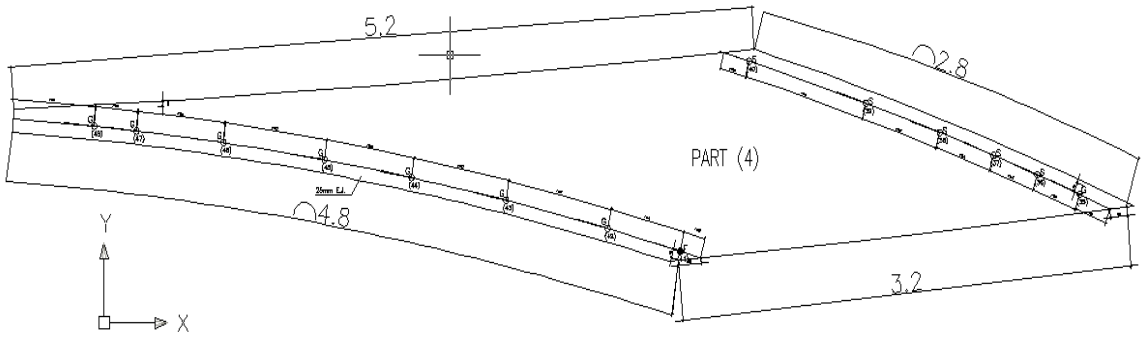

Figure 4.2 Plan of part 4 skew slab.

Figure 4.3 Formwork of part 4 skew slab

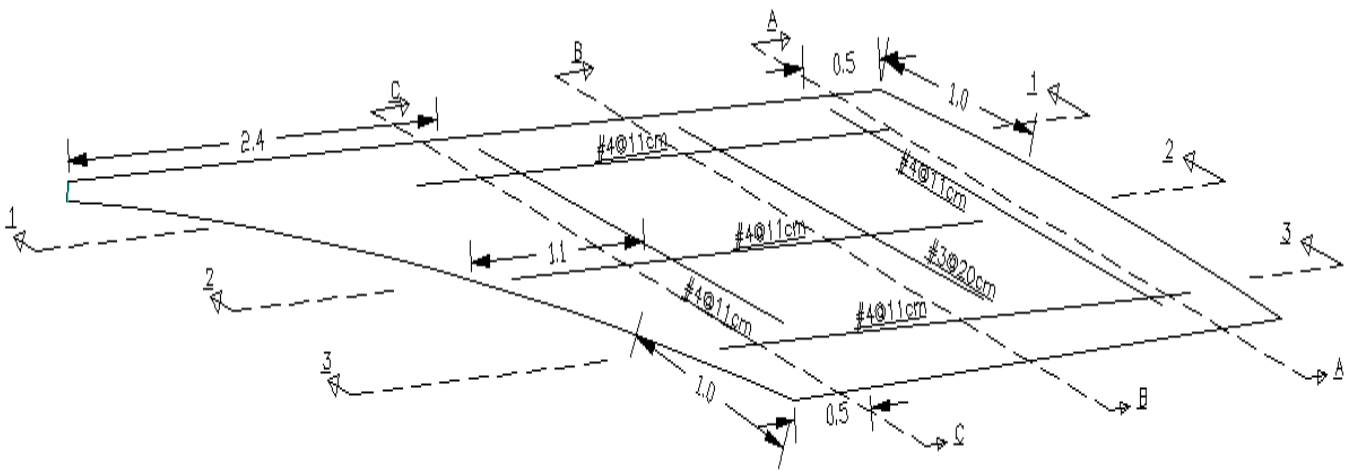

Figure 4.4 Top steel of part 4 skew slab

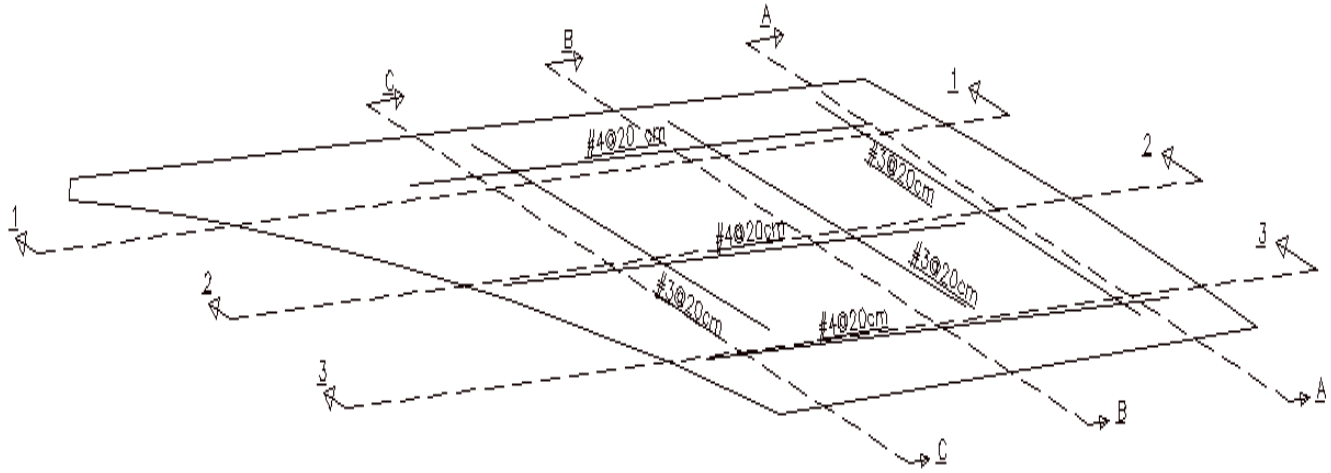

Figure 4.5 Bottom steel of part 4 skew slab

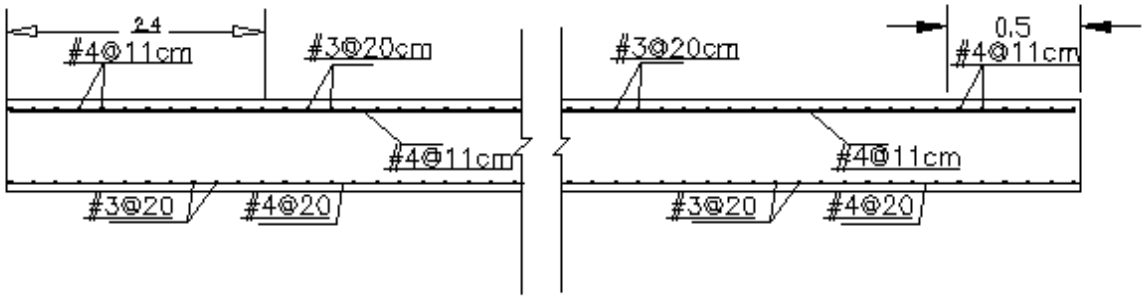

Sec. 1 - 1

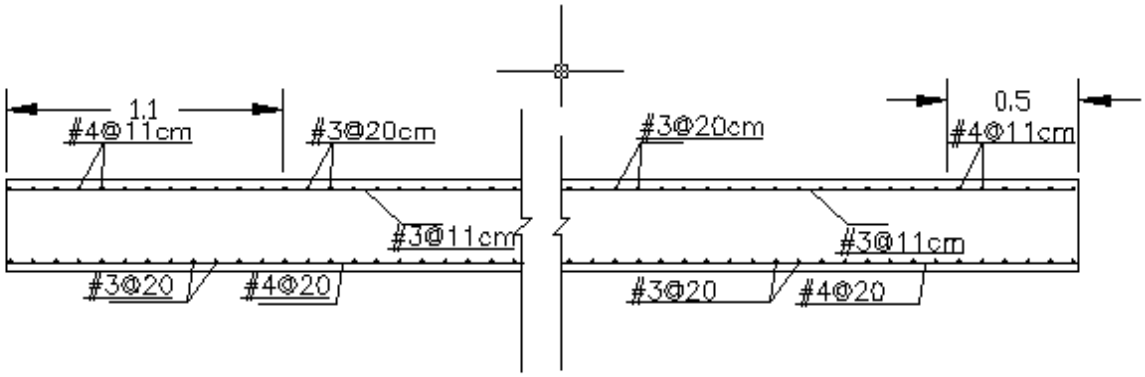

Sec. 2 - 2

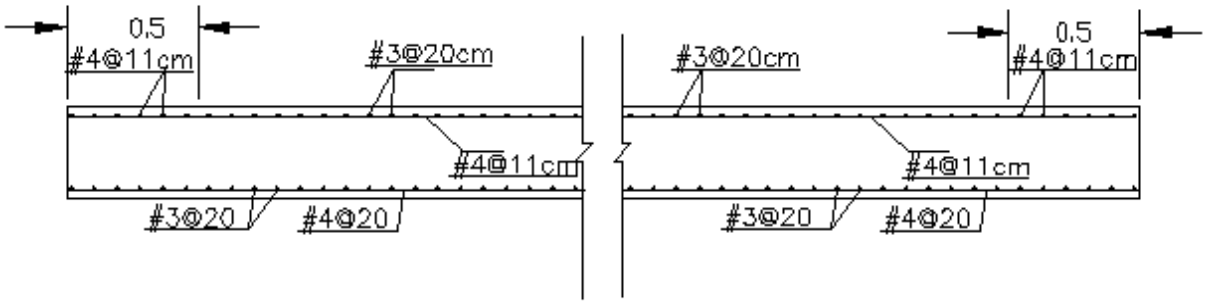

Sec. 3 - 3

Figure 4.6 Longitudinal sections in part 4 skew slab

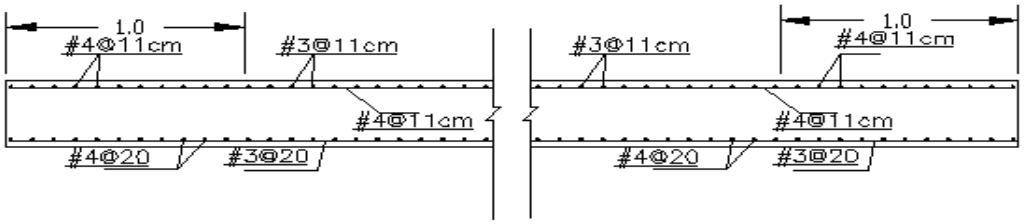

Sec. A - A

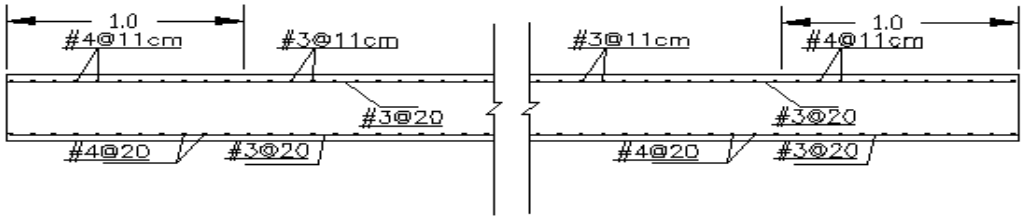

Sec. B - B

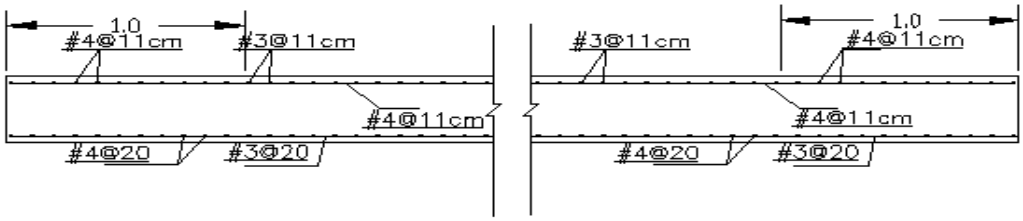

Sec. C - C

Figure 4.7 Perpendicular sections in part 4 skew slab

The steel works of cutting, bending, positioning, Aligning and assembling bars were done by a subcontractor through the details shown befor. Figure 4.8 shows the model when steel works finished.

Figure 4.8 Steel bars inside the formwork

4.5.3 Concrete work

A ready mix company was contracted to supply the required quantity of concrete with strength of 5000 psi, six cylinders (3*6) in^2 were filled when casting the model and then tested after 28 days under compression. the average concrete strength obtained by testing the six cylinders was 33.64 Mpa which equal 4875 psi; this value was used in the analysis. The concrete model has been transported after 28 days of casting from the field to KFUPM lab in building 26 using truck with a crane. Figure 4.9 shows the concrete casting of the model.

4.5.4 Support work

The supports was made of cut pieces of an steel I-beam into 14 pieces same as the support numbers was used to support the model with a (25 cm * 25 cm) area of flange and 35 cm web height. These pieces were placed on leveled floor in the appropriate locations following the locations used in actual structure. Each support was provided with shift rubber pads of (25x25 mm) to simulate the bearings. The deck slab was then placed in position over the supports. The support system was checked to ensure that there was no gap between the support and the slab. Figure 4.10 shows the slab over the supports.

Figure 4.9 Concrete casting of the model

Figure 4.10 Slab model over the supports

4.5.5 Instrumentation

The following instruments were used in the experiment:

a) A load cell,

A load cell of 10 KN maximum capacity and 2.503 coefficient was placed at the location of the maximum reaction expected and provided with shift rubber pad to compare the behavior of that point under loading with FEM analysis. Figures 4.11 shows the load cell used.

b) Electrical strain gauges

A strain gauges of two perpendicular directions (x,y) and 2.11 % coefficient was used in the experiment. The locations of the strain gauges were pointed at the top and the bottom of the slab depending on the maximum stresses expected due to FEM analysis. Beside, these points was cleared and smoothed accurately to blast

the strain gauges. Those strain gauges have been blasted carefully using special blaster and then leaved to the next day to obtain high adhesion strength between them and the model. Figure 4.12 shows the strain gauges.

c) Linear voltage displacement transducers (LVDT)

Linear voltage displacement transducers of 2% coefficient was placed underneath the slab in different locations which have been expected as the locations of the maximum displacements touching the bottom slab face without any gab could affect the readings and checked vertically too. Figure 4.13 shows one of the LVDT used.

Later these gauges have been wired and connected to the data logger using the same wires length for accuracy; the load cell first connected to the first channel and the strain gauges next connected then the LVDT's. Soldering was used to connect the strain gauges to keep the reading from any loading movement; and then the strain gauges have been covered to keep them too from loading. The data logger then has been checked, programmed and initialized to start the loading process. Figure 4.14 shows the portable data logger and wires connection.

Figure 4.15 and 4.16 shows the locations of the strain gauges and LVDT's.

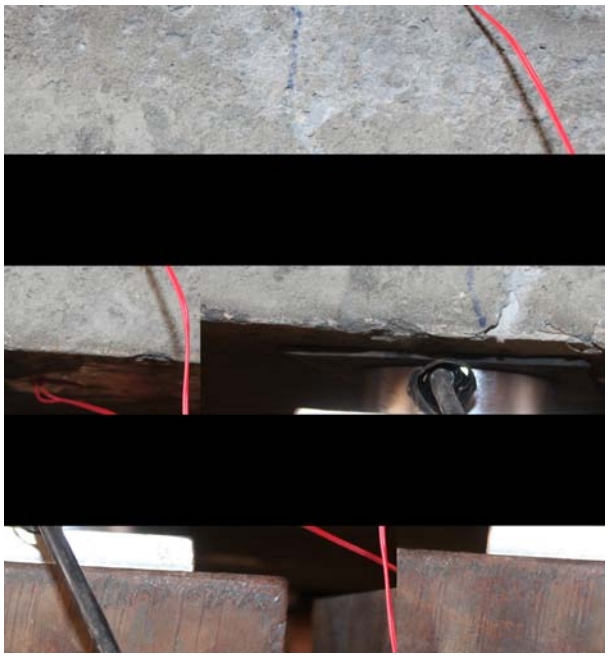

Figure 4.11 Load cell and rubber pad

Figure 4.12 Two perpendicular directions strain gauge

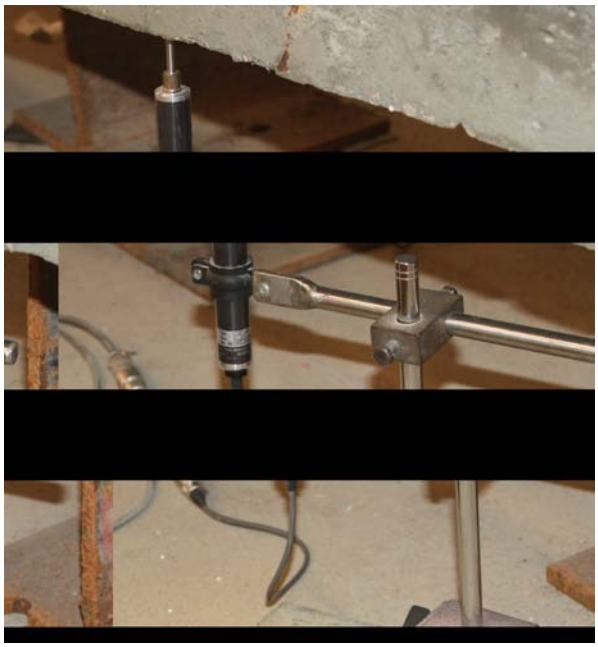

Figure 4.13 Linear voltage displacement transducers (LVDT)

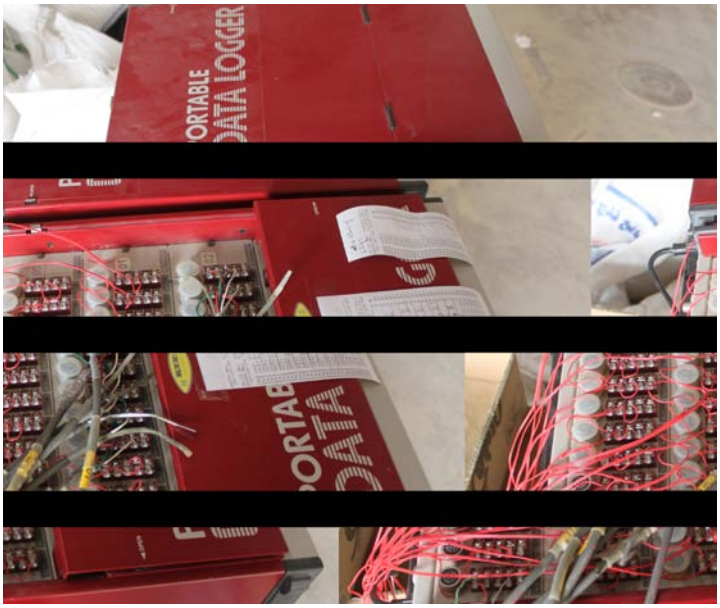

Figure 4.14 Portable data logger

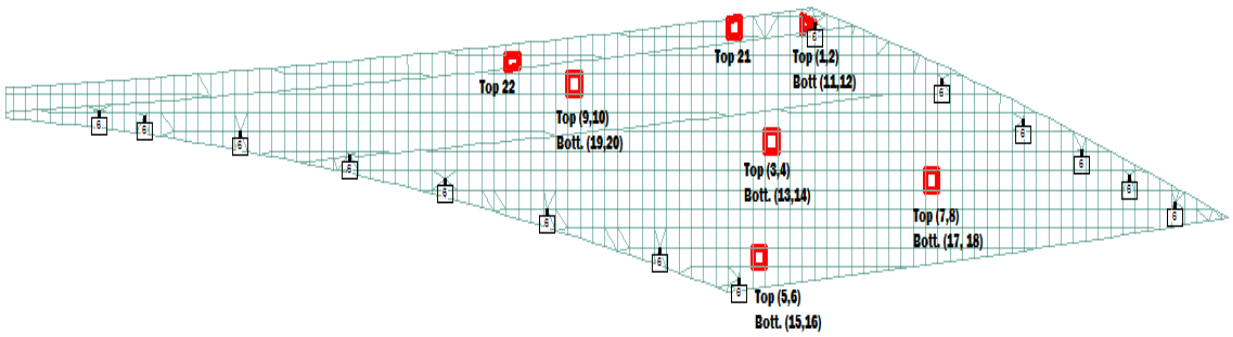

Figure 4.15 Strain gauges locations at the top and bottom

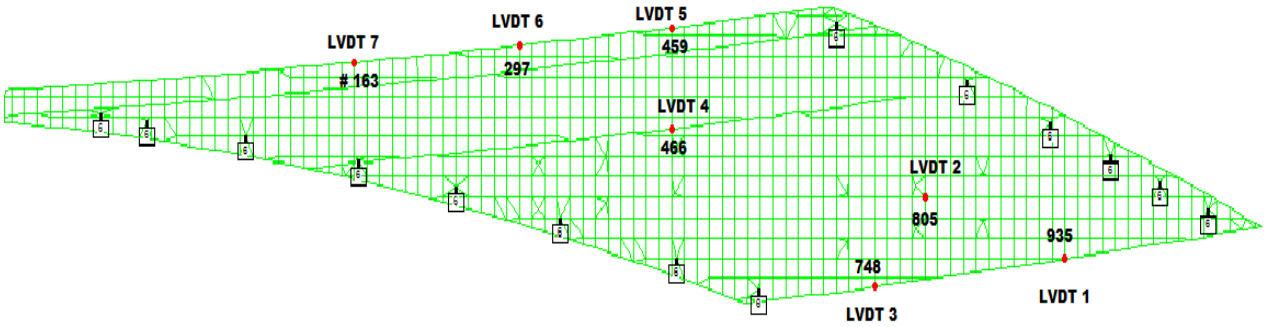

Figure 4.16 LVDT's locations

4.5.6 Loading

Two types of loading were used: a) distributed loading and (b) trucks loading. For distributed loading on the model, wet sand was chosen because it was available in the laboratory and it can be handled. The idea was preparing an empty plastic or carton boxes over the whole model slab to make a uniform loads on the whole area, and then initializing all reading on the data logger to be all zero; then filling a measured amount of sand in that boxes depending on measured height compatible with FEM dead walkway

loads; beside, a different height of sand should be used in the next iteration of loading compatible with FEM dead and live walkway loads to make a proportion of the self weight percentage. The self weight of that slab was neglected and the reading obtained was without self weight values because the gauges were placed after casting that model slab and after placing on the supports.

The weight density of the sand has been measured experimentally and it was 18.14 kN/ m^3

4.5.6.1 Load cases.

Many cases were used for loading process.

1- Uniform load on whole slab (1.20 kN/m^2)

The model was fully loaded by sand with 6.6 cm height uniformly. The carton boxes which used in that loading have been filled by sand at a height of 6.6 cm, this height was found by following;

Edge beam dead load = 0.131 kN/m. See (4.3)

The walkway width = 40 cm = 0.40 m

The load in KN/m^2 = (0.131 kN/m) / (0.40 m) = 0.328 kN/m^2

New Jersey barrier dead load = 0.0775 kN/m . See (4.3)

The load in KN/m^2 = (0.0775 kN/m) / (0.40 m) = 0.194 kN/m^2

Walkway dead load = 0.6 kN/m^2

Now, Total dead loads on the walkway = 0.6 + 0.194 + 0.328

= 1.122 kN/m^2

The walkway area = 2.042 m^2

Load = 1.122 x 2.042 = 2.291 kN

At the first calculations we used sand weight density of 17 kN/m^3

The volume = (2.291 kN) / (17 kN/m^3) = 0.135 m^3

The height = (0.135 m^3) / (2.042 m^2) = 0.066 m

Then, h = 6.6 cm

Now by using the actual weight density calculated (18.14 kN/ m^3)

The load = 0.066 m x 18.14 kN/ m^3 = 1.20 kN/ m^2.

This load has been filled uniformly over the whole slab. Figure 4.17 shows the carton boxes and the sand inside.

2- Uniform load on whole slab (1.741 kN/m^2).

The model was fully loaded by sand with 9.6 cm height uniformly. In this case the boxes have been filled by sand at a height of 9.6 cm, this height was found by following;

Total dead loads on the walkway = 1.122 kN/m^2

Walkway live load = 0.52 kN/m^2. See (4.3)

Total loads = 1.122 + 0.52 = 1.624 kN/m^2

The height = (1.624 kN/m^2) / (17 kN/ m^3) = 0.096 m

Then, h = 9.6 cm

Now by using the actual weight density calculated (18.14 kN/ m^3)

The load = 0.096 m x 18.14 kN/ m^3 = 1.741 kN/ m^2.

This load has been filled uniformly over the whole slab. Figure 4.18 shows the carton boxes and the sand inside.

3- Walkway dead and live loads at 9.6 cm height (1.741 kN/m^2).

4- Walkway dead and live loads at 9.6 cm height with two trucks. (case 1)

5- Walkway dead and live loads at 9.6 cm height with two trucks in different location. (case 2)

6- Walkway dead and live loads at 9.6 cm height with two trucks in different location. (case 3)

7- Walkway dead and live loads at 9.6 cm height with two trucks in different location. (case 4)

Figures (4.19 – 4.22) show the walkway and live load cases

.

Figure 4.17 Carton boxes with sand inside at 6.6 cm

Figure 4.18 Carton boxes with sand inside at 9.6 cm

Figure 4.19 Walkway loads at 9.6 cm height with two trucks

Figure 4.20 Walkway loads at 9.6 cm height with two trucks

Figure 4.21 Walkway loads at 9.6 cm height with two trucks

Figure 4.22 Walkway loads at 9.6 cm height with two trucks

CHAPTER FIVE

THEORETICAL STUDY OF MODEL BRIDGE

5.1 General

This approach discretizes the structure into small divisions (elements) where each element is defined by a specified number of nodes. The behavior of each element (and ultimately the structure) is assumed to be a function of its nodal quantities (displacements and/or stresses), that serve as the primary unknowns in this formulation. This is one of the most general and accurate methods to use, because it does not put any limitation on the geometry, loads, or boundary conditions, and can be applied to open/closed girders and static/dynamic analysis. Additionally, the structure's response can always be improved by refining the mesh and increasing the number of nodes (or degrees of freedom) for each element. However, the rather involved modeling and analysis efforts required by this method may in some cases make it impractical for preliminary analysis

5.2 Modeling of the Bridge Deck

The present study is related to the Part 4 slab of the bridge. For analysis and design check of the Part 4 of the curved bridge, a finite element model of the slab of the Part 4 of the existing bridge was developed using Structural Analysis and Design Software STAAD Pro 2007.

The Part 4 of the slab bridge is supported on six pot bearings spaced at varying distances on the North-East abutment and eight pot bearings on the South-West abutment as shown in the Figure 5.1.

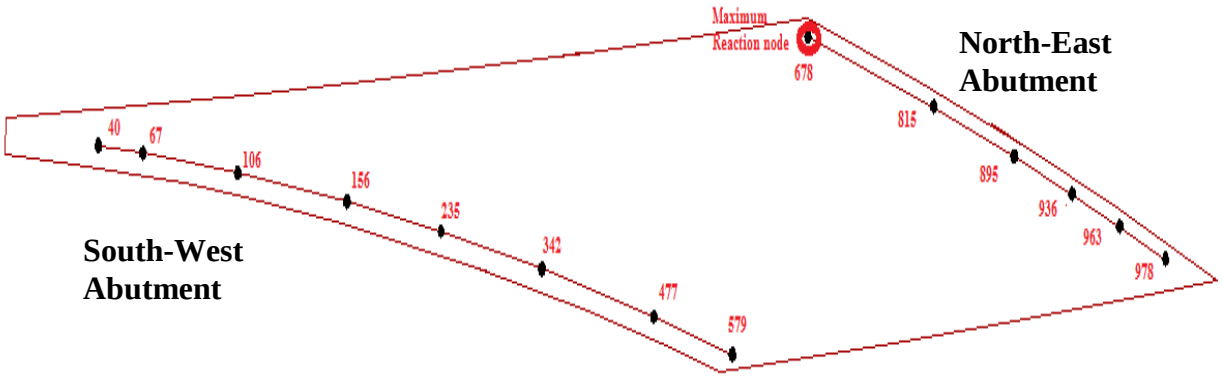

Figure 5.1 Location of bearings (Support) on the Abutment

The finite element model of the slab is shown in Figure 5.2. The finite element mesh is 0.08m x 0.08m in size. The aspect ratio of the elements is 1 or less. The lines parallel to the roadway in the mesh indicates the boundary of the walkway and the barrier line. These lines have been placed to apply the barrier loads and the walkway loads on the slab. The finite element model comprises 976 elements and 992 nodes. Plate elements are used for modeling the slab and the thickness of the plate is assigned as 0.1 m.

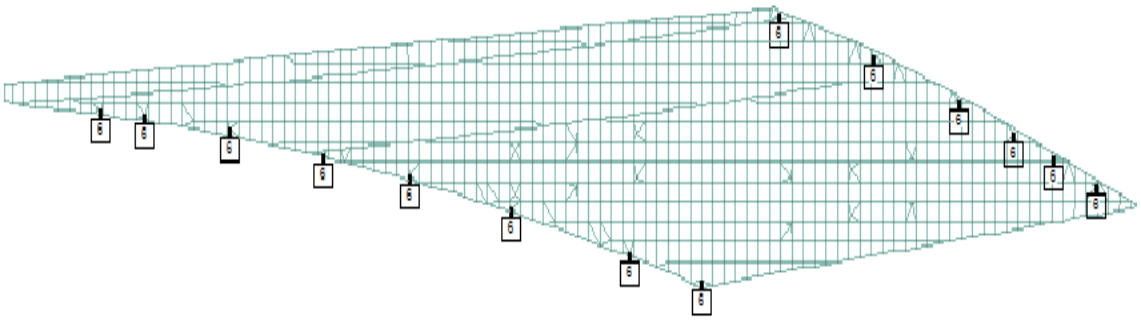

Figure 5.2 Finite element mesh of the Part 4 of the slab bridge

5.3 Loads on the Slab Deck

5.3.1 Dead Load

- Self weight of 1m reinforced concrete slab has been scaled 1/10 to be 0.1m.
- Self weight of 0.3 m x 1.75 m edge beam has been scaled to 1/1000.
- New Jersey barrier weight = 0.31 m^2 has been scaled to 1/1000.
- Weight of the walkway dead loads = 25 kN/m^3 x 0.25 m = 6.0 kN/m^2 has been scaled to 1/10, which is equal 0.60 kN/m^2.
- Live load on walkway = 5.2 kN/m^2 has been scaled to 1/10, which is equal 0.52 kN/m^2 .

  By calculating the dead loads, the total dead loads when scale down was 1.22 kN/m^2

  The total loads = 1.22 + 0.52 = 1.74 kN/m^2 which was used in FEM work.

5.3.2 Live Load

A scaled walkway live load of 0.52 kN/m^2 is considered for the analysis of the deck slab. The truck load considered in the design is the standard truck as per Ministry of Communication, Saudi Arabia recommendations. The scaled live load for the MOC truck consists of a leading load of 0.04 kN/wheel followed by two loads at 0.43 m spacing with a scaled value of 0.13 kN/wheel. The concentrated truck loads are shown in Figure 5.3 and the MOC truck is shown in Figure 5.4 and 5.5. The live load can be placed on any location of the deck slab. A typical live load position of the trucks is shown in Figure 5.6.

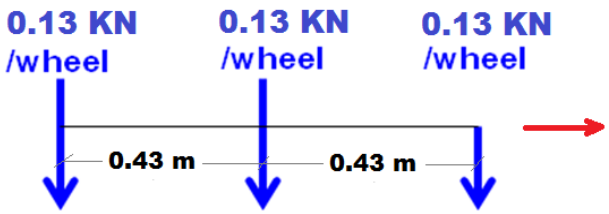

Figure 5.3 Loading configuration of MOC truck (Truck Loads)

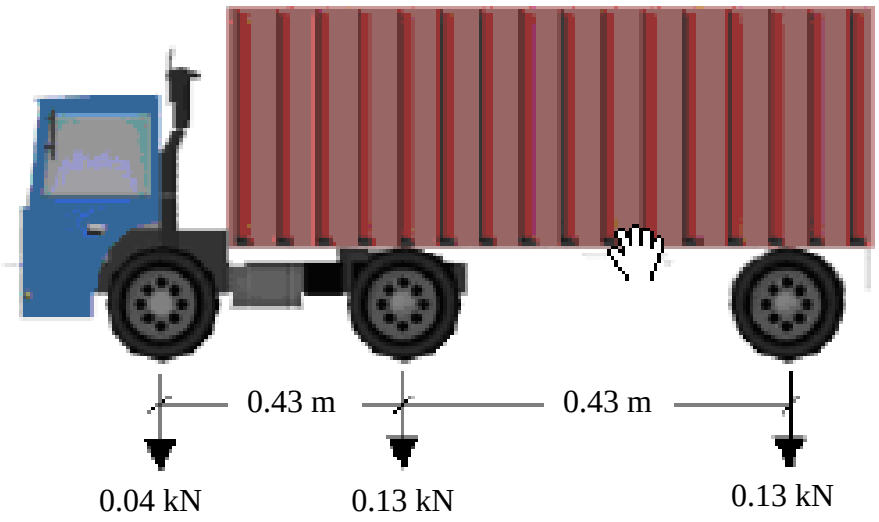

Figure 5.4 MOC truck (Truck Load)

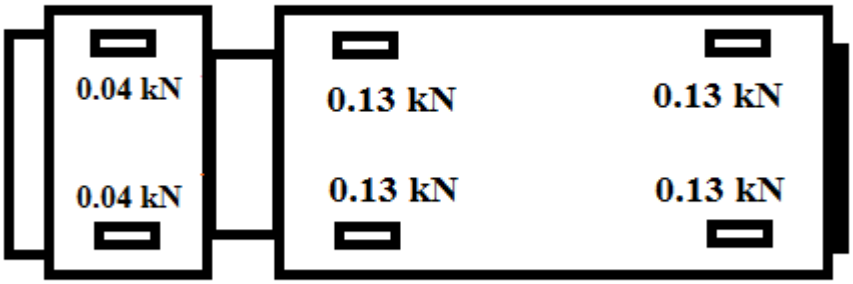

Figure 5.5 Plan view of MOC truck (Truck Load)

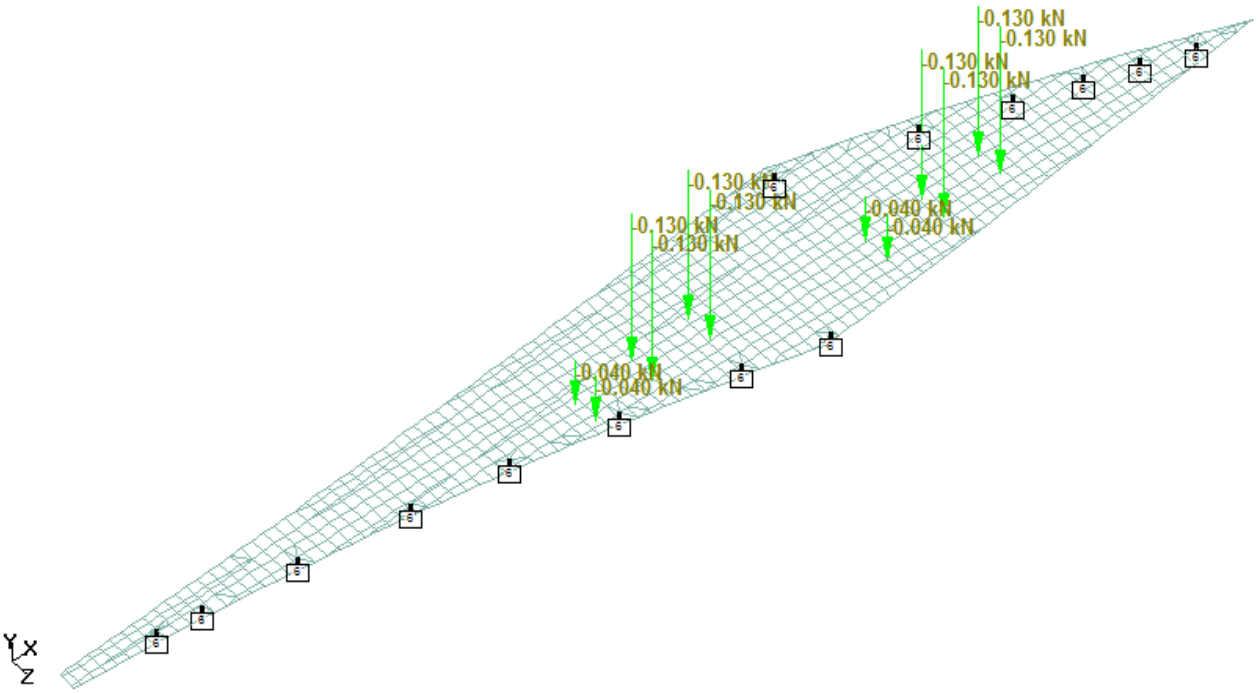

Figure 5.6 Typical Live load Position on the Deck (Truck Load)

CHAPTER SIX

RESULTS AND DISCUSSION

6.1 General

The model slab bridge is 0.1 m thick and the superimposed dead loads including the walkway, barrier and edge beam constitute a major chunk of the load on the structure. Since the prototype underwent deflection and cracking under the self weight it was important to check the bridge under the dead loads. The results of dead and live loads analysis of prototype, theoretical model and experimental model are presented in this Section.

6.2 Model Results and Prototype

6.2.1 Results due to self weight

The reactions at the supports are shown in Table 6.1 due to the self weight. It shows that reaction scale is (1/1000) which is expected for this study.

Node	Prototype Reactions (kN)	Model Reactions (kN)
40	483.635	0.476
58	67.681	0.079
102	634.647	0.628
173	835.695	0.848
249	1021.222	1.001
351	1421.376	1.435

477	450.413	0.449
578	1835.476	1.832
679	3011.272	3.014
849	390.057	0.38
917	850.957	0.872
959	416.356	0.388
986	249.908	0.27
1006	220.007	0.214

Table 6.1 Reactions due to self weight for the model and prototype

The deflections are shown in Table 6.2 due to the self weight. It shows that deflection scale is (1/100) which is expected for this study.

Node	Prototype Deflection (mm)	Model Deflection (mm)
310	-40.383	-0.404
459	-30.703	-0.307
606	-6.278	-0.063
648	-7.316	-0.073
748	-14.562	-0.133
885	-19.226	-0.194
979	-9.526	-0.107
163	-31.55	-0.315

Table 6.2 Deflections due to self weight for the model and prototype

The stresses are shown in Table 6.3 due to the self weight. It shows that deflection scale is (1/10) which is expected for this study.

Plate	Prototype Stress (N/mm2)	Model Stress (N/mm2)
664	7.636	0.839
624	5.185	0.52
597	5.162	0.518
472	5.079	0.507
624	4.063	0.409
597	3.18	0.319
472	2.126	0.213
832	2.078	0.208
664	0.79	0.105
832	0.391	0.039

Table 6.3 Stresses due to self weight for the model and prototype

6.2.2 Results due to walkway load

The reactions at the supports are shown in Table 6.4 due to walkway load.

The actual uniform load is 17.41 kN/m^2

The model uniform load is 1.741 kN/m^2.

It shows that reaction scale is (1/1000) which is expected for this study.

Node	Prototype Reaction (kN)	Model Reaction (kN)
40	252.098	0.233
58	52.293	0.079
102	784.047	0.778
173	935.654	0.933
249	0	0
351	0	0
477	0	0
578	0	0
679	1534.248	1.533
849	0	0
917	0	0
959	0	0
986	0	0
1006	0	0

Table 6.4 Reactions due to walkway load for the model and prototype

The deflections are shown in Table 6.5 due to walkway load. It shows that deflection scale is (1/100) which is expected for this study.

Node	Prototype Deflection (mm)	Model Deflection (mm)
310	-109.65	-1.097
459	-81.086	-0.812
606	113.986	1.139
648	51.876	0.519
748	218.702	2.141
885	265.164	2.605
979	315.148	3.106
163	-88.325	-0.882

Table 6.5 Deflections due to walkway load for the model and prototype

The stresses are shown in Table 6.6 due to walkway load. It shows that deflection scale is (1/10) which is expected for this study.

Plate	Prototype Stress N/mm2	Model Stress N/mm2
664	4.431	0.443
624	3.291	0.358
597	2.045	0.205
472	1.906	0.191
624	0.769	0.078
597	0.321	0.034
472	0.195	0.03
832	0.189	0.019
664	0.128	0.013
832	0.083	0.008

Table 6.6 Stresses due to walkway load for the model and prototype

6.3 Model results and Experimental

6.3.1 Support Reactions

The reactions at the supports are shown in Table 6.7 (Refer to Figure 6.1 for support nodes). The huge reaction occurs at the corner of the NE abutment at the extreme NW node # 678. The maximum reaction is different from case to another and it is more than three times the maximum reaction at any other support. This huge reaction at the corner node occurs due to the highly skewed nature of the bridge. Maximum reaction occurs at SW node # 579 in some cases.

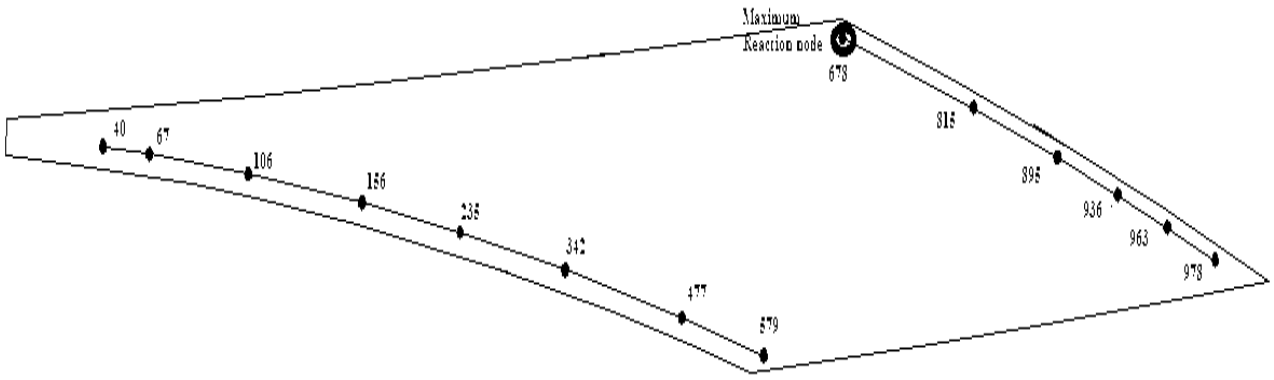

Figure 6.1 Deck slab showing the support nodes

Node	LOAD CASE	Exp. Reaction. Fy (N)	FEM Reaction. Fy (N)
678	Fully Loaded of sand (1.2 kN/m^2)	851	952
678	Fully Loaded of sand (1.741 kN/m^2)	1248	1384
678	Walkway Loaded of sand (1.741 kN/m^2)	1088	1193
678	Walkway Loads + Two trucks c1	1196	1339
678	Walkway Loads + Two trucks c2	1208	1362
678	Walkway Loads + Two trucks c3	1236	1407
678	Walkway Loads + Two trucks c4	1236	1578

Table 6.7 Reactions due to Load Cases on the Slab Bridge

6.3.2 Deflections

Table 6.8 shows the defection at selected locations of the slab bridge. The maximum deflection however occurs in a zone which has side walk 0.4m wide on the long span at the edge. Figure 6.2 shows the nodes at which the deflections are selected and the values of deflection at selected nodes are given in Tables (6.8 - 6.14). Figures (6.3 - 6.9) shows the cases of loading.

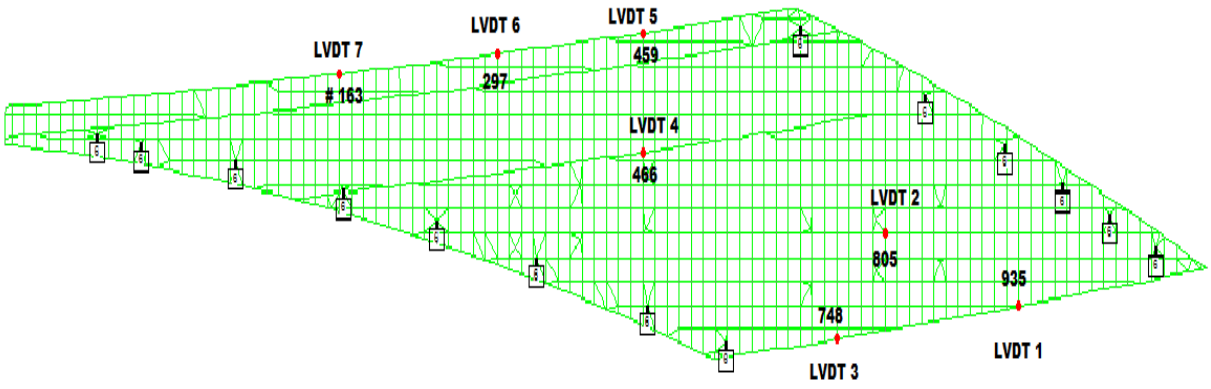

Figure 6.2 Location selected for deflection readings

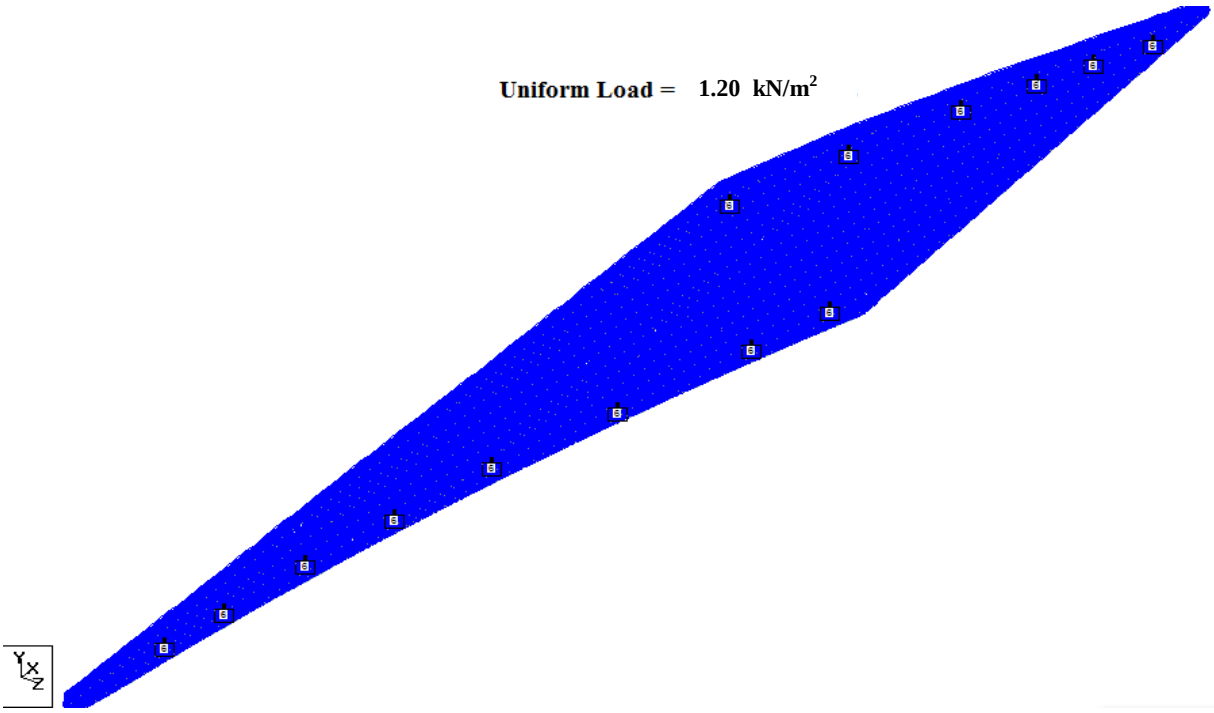

Figure 6.3 Uniform load of sand of (1.20 KN/m^2).

Point	Model Disp. (mm)	FEM Disp. (mm)
1	-0.250	-0.184
2	-0.208	-0.118
3	-0.282	-0.107
4	-0.224	-0.113
5	-0.214	-0.204
6	-0.288	-0.225
7	-0.212	-0.153

Table 6.8 Deflection due to fully loaded by sand of (1.20 kN/m^2).

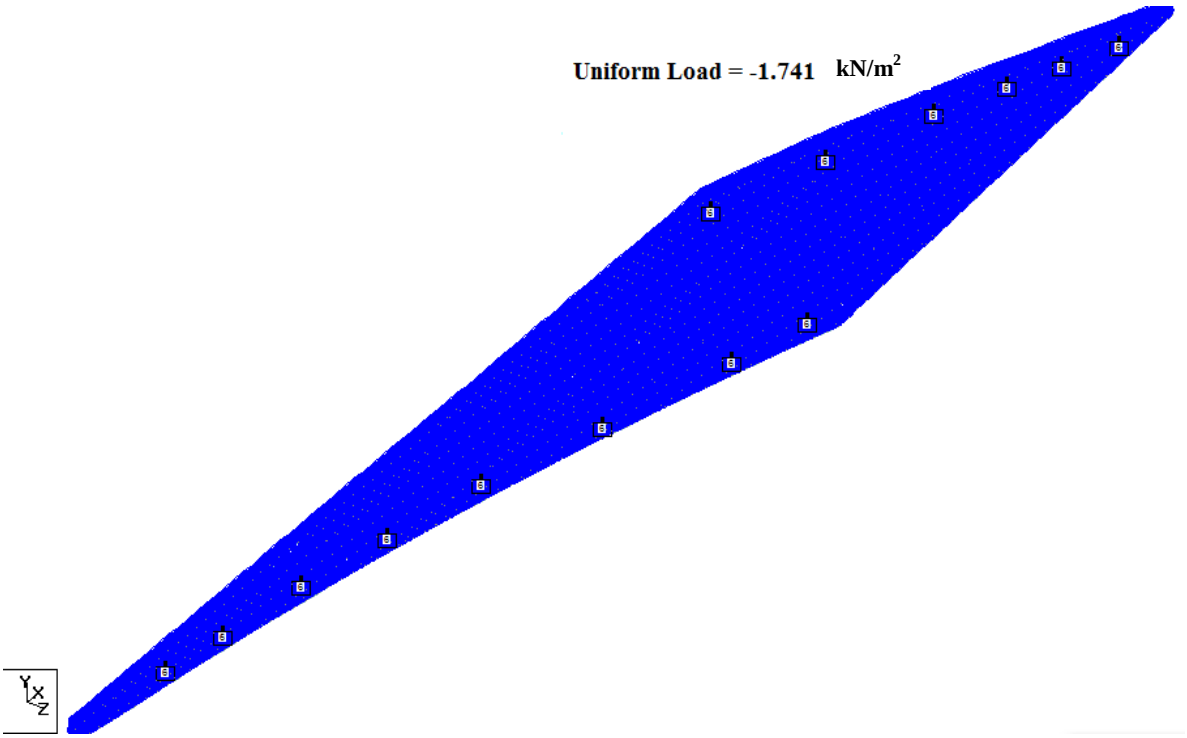

Figure 6.4 Uniform load of sand of (1.741 kN/m^2).

Point	Model Disp. (mm)	FEM Disp. (mm)
1	-0.292	-0.267
2	-0.230	-0.172
3	-0.284	-0.156
4	-0.266	-0.164
5	-0.268	-0.297
6	-0.300	-0.327
7	-0.284	-0.223

Table 6.9 Deflection due to fully loaded by sand of (1.741 kN/m^2).

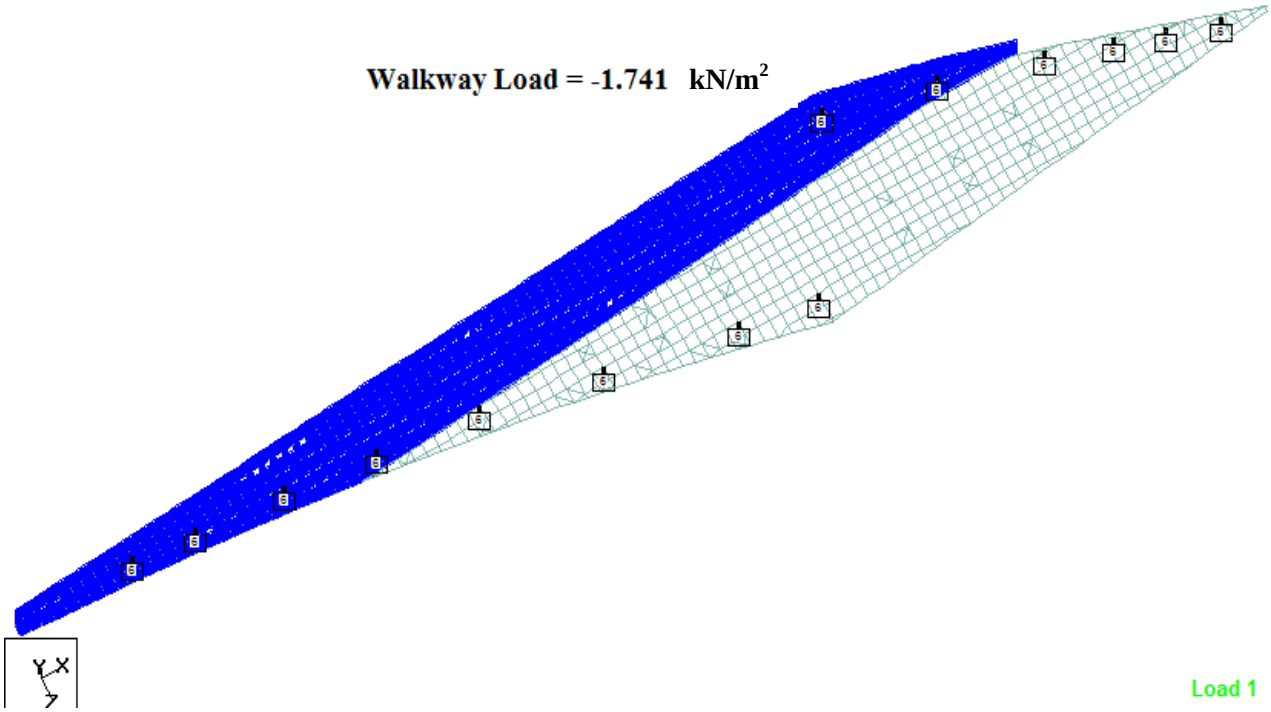

Figure 6.5 Walkway uniform load of sand of (1.741 kN/m^2).

Point	Model Disp. (mm)	FEM Disp. (mm)
1	+0.006	+1.200
2	+0.048	+0.759
3	+0.068	+0.892
4	-0.222	-0.021
5	-0.326	-0.373
6	-0.390	-0.461
7	-0.376	-0.348

Table 6.10 Deflection due to walkway when loaded by sand of (1.741 kN/m^2).

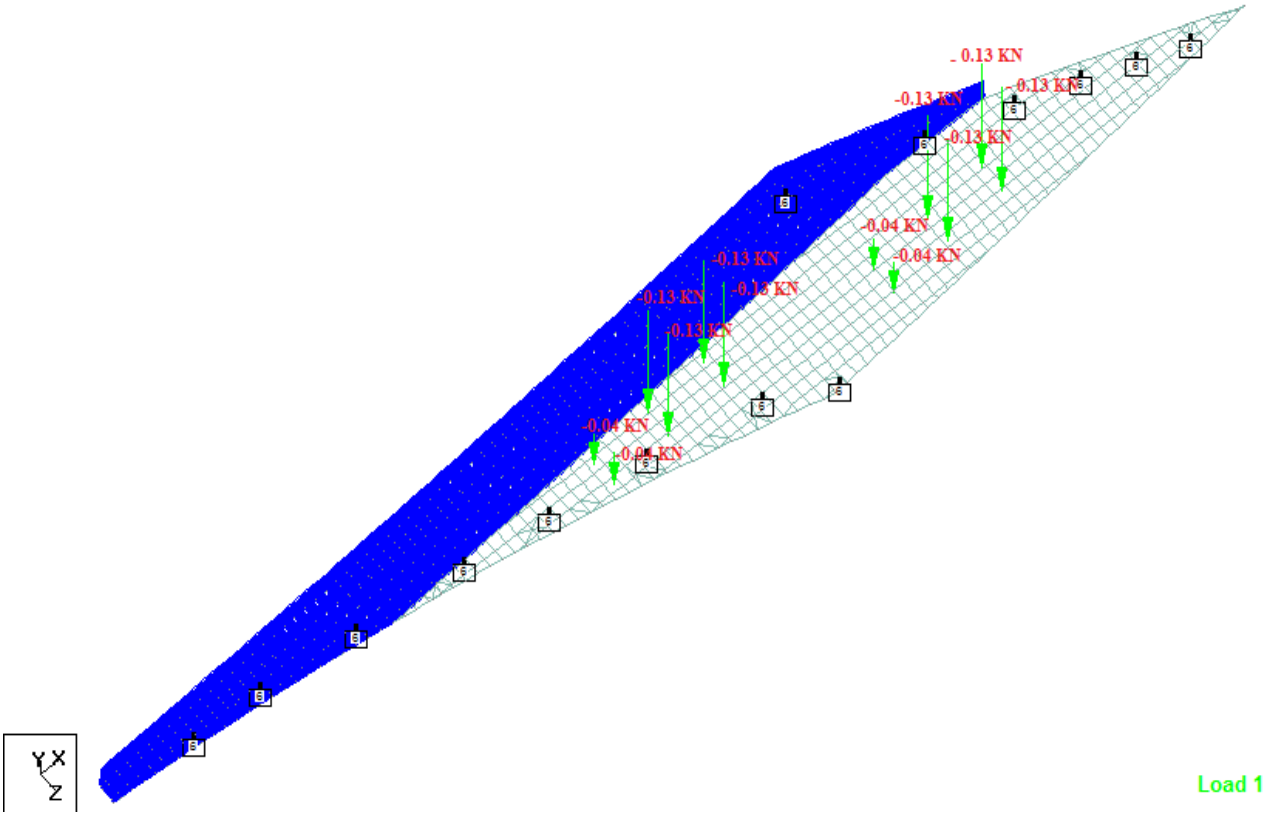

Figure 6.6 Walkway uniform load and trucks loads case 1

Point	Model Disp. (mm)	FEM Disp. (mm)
1	-0.102	-0.064
2	-0.056	-0.047
3	-0.070	-0.046
4	-0.268	-0.162
5	-0.342	-0.325
6	-0.384	-0.415
7	-0.350	-0.329

Table 6.11 Deflection due to walkway loads and trucks loads case 1

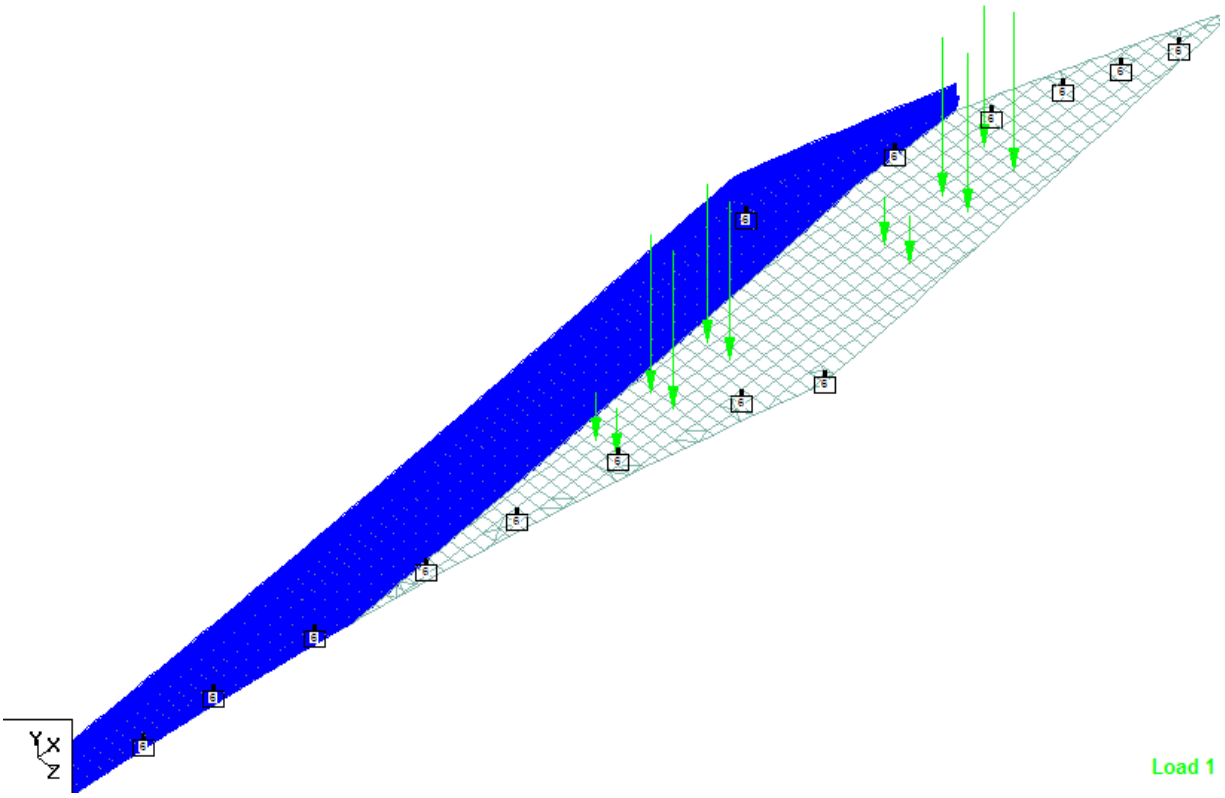

Figure 6.7 Walkway uniform load and trucks loads case 2

Point	Model Disp. (mm)	FEM Disp. (mm)
1	-0.134	-0.071
2	-0.070	-0.042
3	-0.082	-0.037
4	-0.268	-0.165
5	-0.332	-0.331
6	-0.370	-0.418
7	-0.346	-0.330

Table 6.12 Deflection due to walkway loads and trucks loads case 2

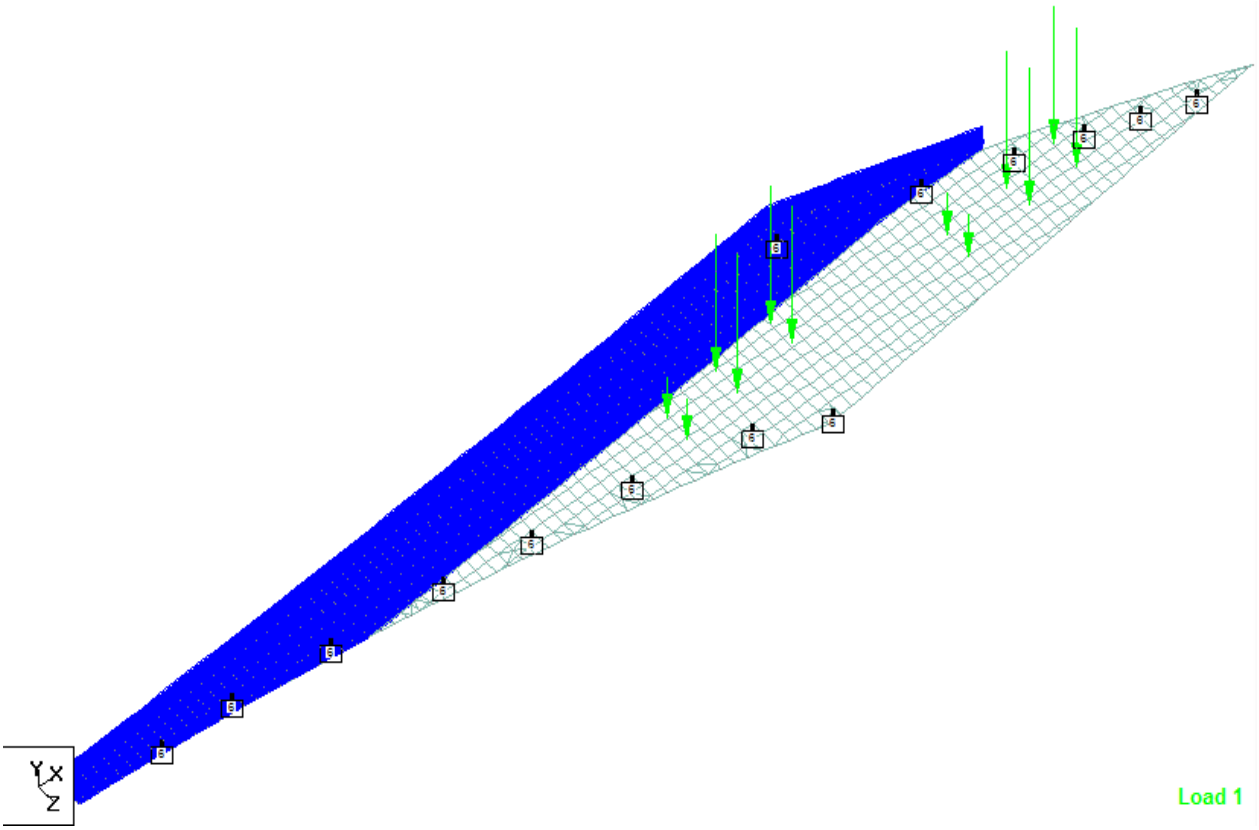

Figure 6.8 Walkway uniform load and trucks loads case 3

Point	Model Disp. (mm)	FEM Disp. (mm)
1	-0.142	-0.048
2	-0.074	-0.011
3	-0.074	+0.001
4	-0.246	-0.173
5	-0.316	-0.347
6	-0.352	-0.429
7	-0.338	-0.337

Table 6.13 Deflection due to walkway loads and trucks loads case 3

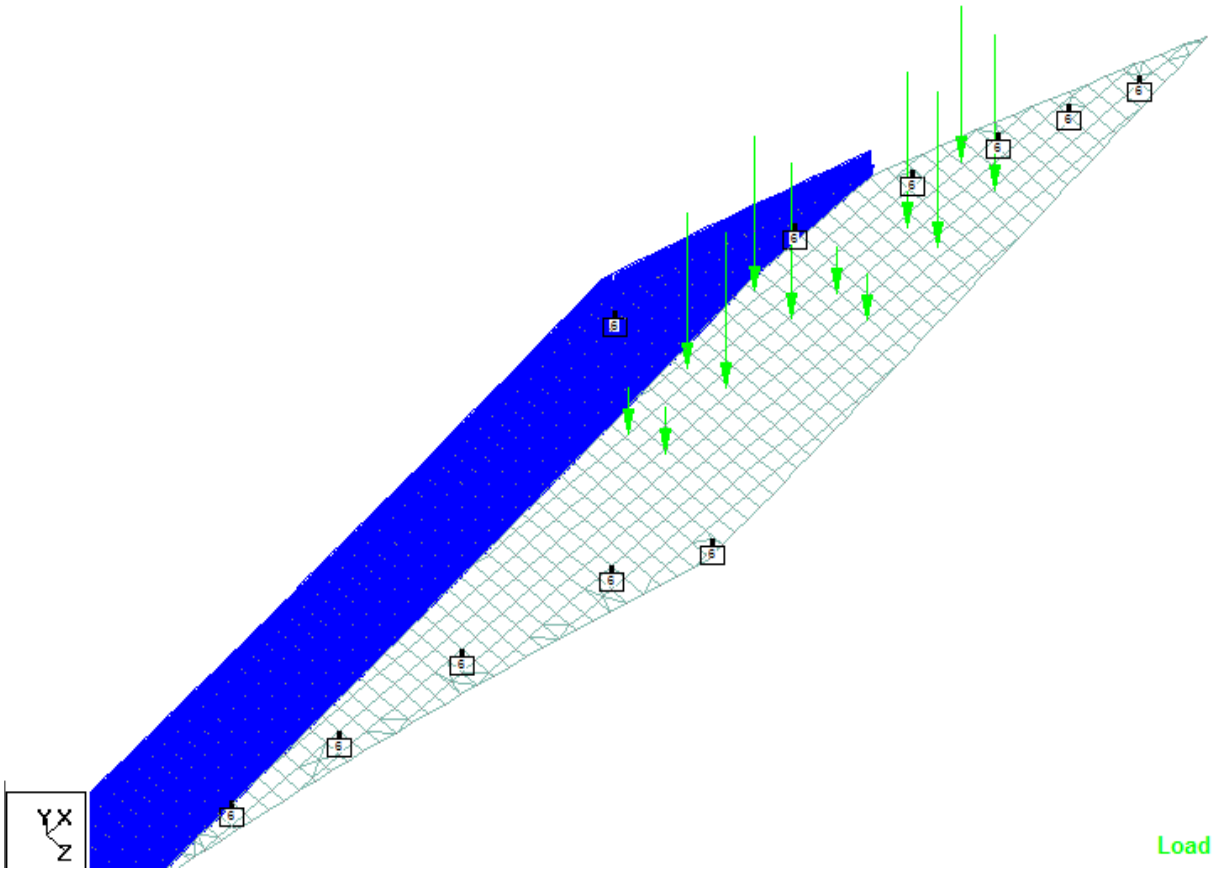

Figure 6.9 Walkway uniform load and trucks loads case 4

Point	Model Disp. (mm)	FEM Disp. (mm)
1	-0.180	-0.086
2	-0.102	-0.058
3	-0.090	-0.065
4	-0.218	-0.124
5	-0.274	-0.254
6	-0.318	-0.334
7	-0.322	-0.269

Table 6.14 Deflection due to walkway loads and trucks loads case 4

6.3.3 Stresses

Table 6.15 shows the stresses at selected locations of the slab bridge. Figure 6.10 shows the plates at which the stresses are selected and the values of stresses at selected plates are given in Tables (6.15 - 6.21). Figures (6.3 - 6.9) shows the cases of loading. In general, except for a few locations, both computed and measured stresses are small. It should be noted that the model stresses are of the order of one-tenth of the values in prototype.

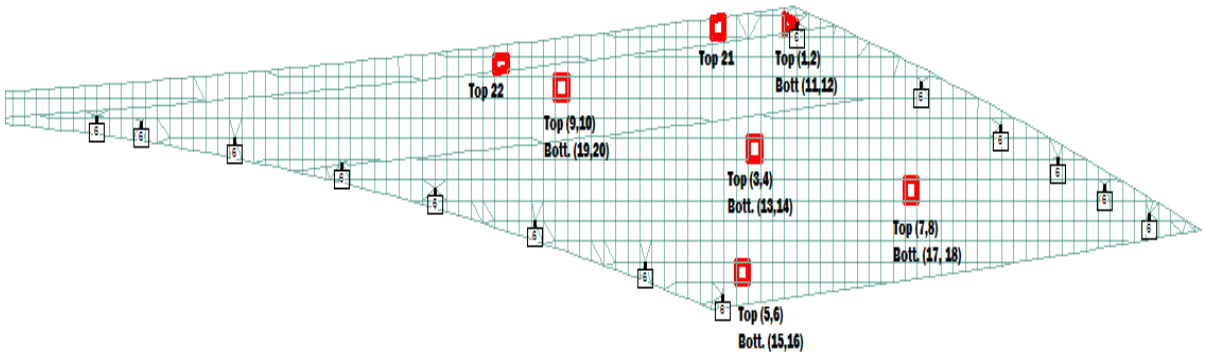

Figure 6.10 Plates at which the stresses are selected

Point		Model Strains 10^{-6} (mm/mm)	Model Stresses (Mpa)	FEM Stresses (Mpa)
		Top		
1	εx	14	0.412	0.272
2	εy	26	0.635	0.034
3	εx	6	0.161	0.164
4	εy	7	0.179	0.203
		Bottom		
11	εx	8	0.202	0.164
12	εy	6	0.165	0.203

Table 6.15 Stresses due to fully loaded by sand of (1.20 kN/m^2).

Point		Model Strains 10^{-6} (mm/mm)	Model Stresses (Mpa)	FEM Stresses (Mpa)
		Top		
1	εx	22	0.823	0.399
2	εy	87	2.029	0.050
3	εx	6	0.168	0.239
4	εy	9	0.224	0.295
		Bottom		
11	εx	16	0.381	0.239
12	εy	6	0.195	0.295

Table 6.16 Stresses due to fully loaded by sand of (1.741 kN/m^2).

Point		Model Strains 10^{-6} (mm/mm)	Model Stresses (Mpa)	FEM Stresses (Mpa)
		Top		
1	εx	21	0.819	0.306
2	εy	92	2.137	0.028
7	εx	16	0.373	0.005
8	εy	4	0.150	0.011

Table 6.17 Stresses due to walkway load (1.741 kN/m^2).

Point		Model Strains 10^{-6} (mm/mm)	Model Stresses (Mpa)	FEM Stresses (Mpa)
		Top		
1	εx	19	0.775	0.432
2	εy	92	2.130	0.037
7	εx	13	0.306	0.014
8	εy	4	0.139	0.068
		Bottom		
11	εx	7	0.183	0.197
12	εy	7	0.183	0.137

Table 6.18 Stresses due to load case 1

Point		Model Strains 10^{-6} (mm/mm)	Model Stresses (Mpa)	FEM Stresses (Mpa)
		Top		
1	εx	9	0.517	0.436
2	εy	83	1.891	0.038

Table 6.19 Stresses due to load case 2

Point		Model Strains 10^{-6} (mm/mm)	Model Stresses (Mpa)	FEM Stresses (Mpa)
		Top		
1	εx	5	0.405	0.453
2	εy	77	1.741	0.035
		Bottom		
9	εx	13	0.314	0.420
10	εy	6	0.184	0.107

Table 6.20 Stresses due to load case 3

Point		Model Strains 10^{-6} (mm/mm)	Model Stresses (Mpa)	FEM Stresses (Mpa)
		Top		
1	εx	11	0.573	0.389
2	εy	86	1.965	0.049

Table 6.21 Stresses due to load case 4

CHAPTER SEVEN

CONCLUSIONS AND RECOMMENDATIONS

7.1 Conclusions

A linear elastic analysis of the skewed deck slab was carried out using a finite element modeling of the slab and all applicable loadings and was carried out using a scaled model too. Based on the findings of this study, the following conclusions are drawn.

1. The skewed slab geometry has contributed to the development of high torsional moment throughout the deck slab. This, in combination with the bending moments in two orthogonal directions, has resulted in high principal moments

2. The computed load deflections of the slab correspond reasonably well with the deflection of the scaled model measured in the lab. The maximum load deflection is at the same location through FEM results and experiment work which is at 2.0 m from the point of maximum reaction of the long span 5.2 m.

3. A reasonably good correlation between the experimental results and the theoretical results of the model was noted. The agreement was much closer with respect to deflection. The measured reaction at the N-W corner also matched reasonably well with the theoretical values. With respect to stresses, the correlation was not as good as expected.

4. The scaled model test is useful to understand the behavior and response of the actual structure and can serve as a useful technique to verify analytical prediction.

7.2 Recommendations

Based on the geometry of the structural condition of the model slab, the following recommendations are made:

1. Designing of such deck slabs with high skew and irregular geometry is not recommended because of complex structural behavior.

REFERENCES

[1] Adel Fam, Hank Huitema and Derk Meyer, “Design of Highly Curved Concrete Ramp Bridges”. 2006.

[2] American Association of State Highway and Transportation Officials (1996). “AASHTO Standard Specifications for Highway Bridges”. 16th Edition. Washington, D.C.

[3] Cagri Ozgur and Don White, “Behavior and Analysis of a Curved and Skewed I-Girder Bridge”. 2008.

[4] Elizabeth K. Norton, “Response of a Skewed Composite Steel-Concrete Bridge Floor-System to Placement of the Deck Slab”. Master Thesis, The Pennsylvania State University, August 2001.

[5] J. A. Sato, F. J. Vecchio, and H. M. Andre, “Scale-Model Testing of Reinforced Concrete under Impact Loading Conditions”. 1987.

[6] Maher Shaker Qaqish, “Effect of Skew Angle on Distribution of Bending Moments in Bridge Slabs”. Journal of Applied Sciences 6 (2): 366-372, 2006.

\[7] Md. Khasro Miah and Ahsanul Kabir, “A Study on Reinforced Concrete Skew Slab Behavior”. 2005.

[8] S. (Sri) Sritharan, Akira Igarashi, M.J. Nigel Priestley, and Frieder Seible, “Test Design of the PRESSS Five-Story Precast Concrete Building”. 1999.

[9] W. G. Corley, J. E. Carpenter, H. G. Russell, N.W. Hanson, A. E. Cardenas, T. Helgason, J. M. Hanson, and E. Hognestad, “Construction and Testing of l/10-Scale Micro-Concrete Model of New Potomac River Crossing, l-266”. 1975.

[10] Al-Kabani Construction Group Inspectech Report, “ Al-Awali Bridge Tests In Makkah”. December 2008 and January 2009.

[11] KFUPM Civil Engineering Department Report, “An Assessment and Evaluation of Structural Design of Al-Awali Bridge in Makkah”. November (2009) and March 2010.

VITAE

Name Farhat Abdul-Munim Isaili

Nationality Palestinian

Date of Birth 1st November 1982

Present Address KSA, Western, AL Dammam

Permanent Address Palestine, West bank, Hebron

Email Address eng_farhat_civil@hotmail.com

eng_farhat_civil@yahoo.com

Mobile No. +966- 509315762 , +970-599820930

Education

University Obtained B.E in Civil Engineering from Palestine Polytechnic University (PPU), Palestine, 2006

Obtained M.S in Structural Engineering from King Fahd University of Petroleum and Minerals (KFUPM), Dhahran, KSA, 2011.

Work Experience

2006 to 2007 worked as a structural designer and field observer in Abu Hadeid Company for General Trade and Contracting, Hebron, Palestine.

Major Achievements and Awards

Received second Honor Awards in most semesters in the BS program.

Obtained a good GPA (3.30/4.00) among the graduate Civil and Applied Civil Engineering students.